Journal of Inclusion Phenomena and Macrocyclic Chemistry (2022) 102:1–33
https://doi.org/10.1007/s10847-021-01112-3

REVIEW ARTICLE

Lanthanide complexes with polyaminopolycarboxylates as prospective NMR/MRI diagnostic probes: peculiarities of molecular structure, dynamics and paramagnetic properties

Eugeny N. Zapolotsky[1] · Yanyang Qu[2] · Sergey P. Babailov[1]

Received: 13 August 2021 / Accepted: 5 October 2021 / Published online: 11 November 2021

Abstract
The paramagnetic lanthanide complexes with polyaminopolycarboxylate (PAPC) ligands attract considerable attention from the standpoint of potential applications thereof as relaxation agents used in medical magnetic resonance imaging (MRI) and in luminescent materials, as well as owing to promising use thereof as paramagnetic labels for studying the properties of biopolymers since they exhibit thermodynamic stability, good solubility in aqueous media and moderate toxicity. For the last decades, the NMR methods have been used to determine the physical and chemical properties of paramagnetic Ln compounds. The studies concerning paramagnetic NMR lanthanide-induced shifts (LISs) in dissolved Ln complexes, as well as the analysis of band shape as a function of temperature make it possible to obtain valuable information on the structure, intra- and intermolecular dynamics and paramagnetic properties thereof. This review is devoted solely to the following features: firstly, the processes of intramolecular dynamics of lanthanide complexes with polyamino-polycarboxylate ligands such as DOTA, EDTA and DTPA and their derivatives studied by NMR; secondly, the LISs of lanthanide complexes with EDTA, DOTA, DTPA and some of their derivatives depending on temperature and pH. Moreover, in this review, for the first time, the dependence of the activation energy of molecular dynamics in complexes with polydentate ligands on the atomic number of the lanthanide cation is analyzed and a monotonic change in energy is detected, which is due to the effect of lanthanide contraction. It should be noted that this phenomenon is quite general and may also appear in the future in many other series of lanthanide complexes with both other multidentate ligands and with bidentate and monodentate ligands. In the future, it is possible to predict the dependence of the properties of certain lanthanide complexes on the ionic radius of the lanthanide cation based on the approaches presented in the review. In this review, we have also presented the dynamic NMR as the main research method widely used to analyze the processes of molecular dynamics, and the structural studies based on the NMR relaxation spectroscopy and LIS analysis.

Keywords Lanthanide complexes · DOTA · EDTA · DTPA · NMR/MRI temperature sensor · Lanthanide-induced shifts in NMR spectra · Free energy of activation · Conformation dynamics

Abbreviations

BSA	The band-shape analysis within the framework of dynamic NMR
BSATTD-LIS	Band-shape analysis technique taking into account temperature dependence of LIS
18-Crown-6	1,4,7,10,13,16-Hexaoxacyclo-octadecane
CD	Circular dichroism (the differential absorption of left and right circularly polarized light)
CEST	Chemical exchange saturation transfer
Diaza-18-crown-6	1,10-Diaza-4,7,13,16-tetraoxacyclo-octadecane

✉ Sergey P. Babailov
babajlov@niic.nsc.ru

[1] A.V. Nikolaev Institute of Inorganic Chemistry, Siberian Branch of the Russian Academy of Sciences, Av. Lavrentyev 3, Novosibirsk, Russia 630090

[2] Institute of Chemical Materials, CAEP, P. O. Box 919-311, Mianyang 621900, Sichun, China

DNMR	Dynamic nuclear magnetic resonance
DOTA	1,4,7,10-Tetraaza-1,4,7,10-tetrakis (carboxymethyl) cyclododecane
DOTAM	1,4,7,10-Tetrakis (acetamido) -1,4,7,10-tetraazacyclodecane
DOTMA	(1R, 4R, 7R, 10R) -α, α ', α '', α ‴-tetramethyl-1,4,7,10-tetraazacyclodecane-1,4,7,10-tetraacetic acid
DOTP	1,4,7,10-Tetraazacyclodecane-1,4,7,10-tetramethylphosphonic acid
DSS	Sodium salt of 3-trimethylsilyl-1-propanesulfonic acid
DTPA	Diethylenetriamine-N,N, N',N,N'',N''-pentaacetic acid
EDTA	Ethylenediamine-N,N, N',N'-tetraacetic acid
EPR	Electron paramagnetic resonance
EXSY	Exchange spectroscopy
LIS	Lanthanide-induced shift
Ln	Cation of the lanthanide element
LSR	Lanthanide shift reagents
MCPE	Macrocyclic polyethers
MRI	Magnetic resonance imaging
MT	Selective magnetization transfer method
NMR	Nuclear magnetic resonance
Oep	Octaethylporphyrin
PAPC	Polyamino-polycarboxylate
PARR	Paramagnetic relaxation reagent
Ptfa	1,1,1-Trifluoro-5,5-dimethyl-2,4-hexanedione
REE	Rare earth elements
RS NMR	Relaxation NMR spectroscopy
SST	Spin saturation transfer technique
TETA	1,4,8,11-Tetraazacyclotetradecane-1,4,8,11-tetraacetic acid
Tpp	Tetraphenylporphyrin
T_1	The spin–lattice relaxation time
T_2	The spin–spin relaxation time

Introduction

The paramagnetic lanthanide complexes with polyaminopolycarboxylate (PAPC) ligands attract considerable attention from the standpoint of potential applications thereof as relaxation agents used in medical magnetic resonance imaging (MRI) and in luminescent materials, as well as owing to promising use thereof as paramagnetic labels for studying the properties of biopolymers since they exhibit thermodynamic stability, good solubility in aqueous media and moderate toxicity. For the last decades, the NMR methods have been used to determine the physical and chemical properties of paramagnetic Ln [1–6]. Recently, the structural features, paramagnetic properties, kinetic and energy parameters of the molecular dynamics of reversible processes occurring in Ln complexes dissolved in organic and aqueous media have been determined by using NMR [7–11] concerning paramagnetic NMR lanthanide-induced shifts (LISs) in dissolved Ln complexes, as well as the analysis of band shape as a function of temperature make it possible to obtain valuable information on the structure, intra- and intermolecular dynamics and paramagnetic properties thereof. In this review, we are focusing exclusively on a detailed study of Ln complexes in aqueous solutions. The complexes of Ln with PAPC ligands exhibit common properties: good solubility in aqueous media, thermodynamic and kinetic stability, low toxicity and relatively fast excretion half-time. In particular, lanthanides with such PAPC ligands as DOTA, DTPA and EDTA have been reported [12–14] for using Gd complexes with DOTA and DTPA as contrasting relaxation reagents [15–21]. As shift agents for NMR applications, -diketonate complexes with paramagnetic [22–24] the case of organic media and $[Ln(H_2O)_n$ (EDTA)] [25, 26] the case of aqueous media have been used [27–45]. The analysis of paramagnetic properties such as the temperature sensitivity of LIS and paramagnetic increases in relaxation rates indicates the prospect of using kinetically stable lanthanide complexes as temperature-sensitive probes for determining local temperature and diagnosing diseases (cancer, inflammation, COVID-19) using MRI technologies.

This review is devoted solely to the following features: firstly, the processes of intramolecular dynamics of lanthanide complexes with polyamino-polycarboxylate ligands such as DOTA, EDTA and DTPA and their derivatives studied by NMR; secondly, the LISs of lanthanide complexes with EDTA, DOTA, DTPA and some of their derivatives depending on temperature and pH. Moreover, in this review, for the first time, the dependence of the activation energy of molecular dynamics in complexes with polydentate ligands on the atomic number of the lanthanide cation is analyzed and a monotonic change in energy is detected, which is due to the effect of lanthanide contraction. It should be noted that this phenomenon is quite general and may also appear in the future in many other series of lanthanide complexes with both other multidentate ligands and with bidentate and monodentate ligands. In the future, it is possible to predict the dependence of the properties of certain lanthanide complexes on the ionic radius of the lanthanide cation based on the approaches presented in the review. In this review, we have also presented the dynamic NMR as the main research method widely used to analyze the processes of molecular dynamics, and the structural studies based on the NMR relaxation spectroscopy and LIS analysis. A detailed description of modern methods of magnetic resonance for studying chemical processes is of interest to a wide range

of chemists, in particular, due to the fact that a number of methodological techniques were only used once for specific research [46–50] and are known to a very limited circle of narrow specialists in various scientific disciplines.

Paramagnetic lanthanide-induced shifts (LISs) on ligand nuclei in lanthanide complexes

The studies on the properties of lanthanide-induced shifts (LIS) and paramagnetic relaxation processes of lanthanide complexes in solutions facilitates developing novel NMR methods for studying the structure, molecular dynamics and thermodynamics of compounds with paramagnetic Ln metal core Ln [1, 27, 28, 38]. The theory of pseudocontact contributions to the LIS [30] was successfully used for the structure of paramagnetic compounds in solutions for many years. The methods based on LIS analysis in NMR spectra have been successfully used in determining the structure and molecular dynamics for compounds with lanthanide cations in the case of small molecules and biological systems such as proteins and nucleic acids [31–33]. Modern theoretical investigations are aimed at studying the relationship between LIS and the parameters of crystal field, the symmetry of complexes, the coordination environment, as well as with the "lanthanide compression"; it should be noted that the newest studies concerning the non-isotropic nature of LIS and paramagnetic relaxation diverge from the «classical» theory [29, 45].

The foundations of the theory of lanthanide-induced shifts can be represented in the following form. The chemical shifts observed on the nuclei of the ligand atoms (δ_{obs}) can be presented as the sums of paramagnetic lanthanide-induced shifts (δ_{LIS}) and diamagnetic associative shifts (δ_D):

$$\delta_{obs} = \delta_D + \delta_{LIS}, \quad (1)$$

In most cases, lanthanide-induced shifts are much greater than corresponding diamagnetic ones (10^1–10^2 ppm on the hydrogen nuclei). In the series of isostructural lanthanide complexes, diamagnetic associative shifts (δ_D) can be readily obtained by processing the spectral data for diamagnetic complexes of La or Lu. Lanthanide-induced shifts (δ_{LIS}) in NMR spectra can be expressed as the sum of Fermi-contact shifts (δ_{FC}) and pseudocontact shifts (δ_{PC}):

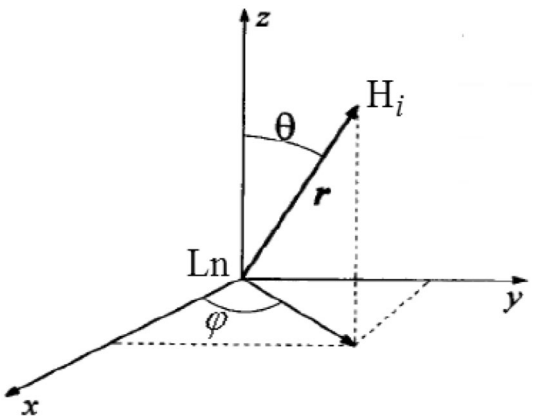

Fig. 1 Spherical coordinates r, θ, φ of the hydrogen nucleus H_i with respect to the Ln cation given in formula (4)

$$\delta_{LIS} = \delta_{FC} + \delta_{PC}, \quad (2)$$

Fermi-contact shifts (δ_{FC}) originate from unpaired s-electron density near the resonant nuclei owing to polarizing completely occupied electron shells in a ligand via the exchange interaction with an incompletely occupied electron shell inherent in a paramagnetic cation. Fermi-contact contributions to the LIS (ppm) are expressed as Eq. (3):

$$\delta_{FC} = \langle S_Z \rangle F, \quad (3)$$

where $< S_Z > = g_J(g_J\text{-}1)J(J+1)$, $F = (A\mu_B/3kT\gamma_I h) \times 10^6$, A is the hyperfine interaction constant in energy units, J is the quantum number of the total angular momentum for the ground state, g_J is the Lande factor associated with this state.

Parameter $< S_Z >$ is characteristic of the Ln cation and independent with respect to the ligand. The value of this parameter for each Ln cation can be found in [7] NMR. Parameter F reflecting relative contact interaction between the Ln cation and the resonant nucleus is unique for each nucleus of the ligand.

In most cases, the Fermi-contact contribution to the LIS is much smaller than the pseudo-contact contributions. Hence, the Fermi-contact contribution can be neglected. Pseudo-contact shifts (δ_{PC}) are caused by the dipole–dipole interaction between the magnetic moment of the resonant nucleus and the magnetic moment associated with the incompletely occupied 4*f*-electron shell of the Ln cation. The pseudo-contact contribution to the LIS

can be expressed with the use of magnetic susceptibility tensor χ (4) [7]:

$$\delta_{PC} = \frac{1}{2N\hbar\gamma}(\overline{\chi} - \chi_{zz})\left\langle \frac{1-3\cos^2\theta}{r^3} \right\rangle + \frac{1}{2N\hbar\gamma}(\chi_{xx} - \chi_{yy})\left\langle \frac{\sin^2\theta\cos 2\phi}{r^3} \right\rangle + \frac{1}{N\hbar\gamma}\chi_{xy}\left\langle \frac{\sin^2\theta\sin 2\phi}{r^3} \right\rangle + \frac{1}{N\hbar\gamma}\chi_{xz}\left\langle \frac{\sin 2\theta\cos\phi}{r^3} \right\rangle + \frac{1}{N\hbar\gamma}\chi_{yz}\left\langle \frac{\sin 2\theta\sin\phi}{r^3} \right\rangle \quad (4)$$

where r, θ, φ are the spherical coordinates of the nucleus with respect to the Ln cation, where r (Å) expresses the distance between the resonant nucleus of the hydrogen atom and the Ln cation, and θ, φ are the angles (Fig. 1).

The right side of expression (4) contains five parameters that describe the case of an arbitrary choice of the principal axes for the magnetic susceptibility tensor of the lanthanide ion with respect to the symmetry axis of the complex [7]. It should be emphasized that the value of the isotropic pseudo-contact contribution expressed by this formula represents originates from averaging over different orientations of the molecule taking into account its motion in the solution. In most cases, no LIS non-isotropy is taken into account, which nevertheless does not hinder any structural studies with satisfactory accuracy [38].

Table 1 The quantum number values of the total angular momentum for ground state J, Lande factor associated with this state g_J, and parameters C_j and $<Sz>$ calculated in [30], among which the latter two characterize, respectively, the paramagnetic pseudo-contact (PC) and Fermi-contact (FC) contributions to the LIS

Ln^{3+}	Type of cation	J	g_J	C_j, %[a]	$<S_z>$, %[b]
Ce^{3+}	$4f^1$	5/2	6/7	− 6.30	− 3.08
Pr^{3+}	$4f^2$	4	4/5	− 11.00	− 9.33
Nd^{3+}	$4f^3$	9/2	8/11	− 4.20	− 14.11
Pm^{3+}	$4f^4$	4	3/5	2.00	− 12.60
Sm^{3+}	$4f^5$	5/2	2/7	− 0.70	0.19
Eu^{3+}	$4f^6$	0	5	4.00	33.56
Gd^{3+}	$4f^7$	7/2	2	0.00	98.99
Tb^{3+}	$4f^8$	6	3/2	− 86.00	100.00
Dy^{3+}	$4f^9$	15/2	4/3	− 100.00	89.72
Ho^{3+}	$4f^{10}$	8	5/4	− 39.00	71.12
Er^{3+}	$4f^{11}$	15/2	6/5	33.00	48.30
Tm^{3+}	$4f^{12}$	6	7/6	53.00	25.80
Yb^{3+}	$4f^{13}$	7/2	8/7	22.00	8.14

[a]Paramagnetic pseudo-contact contributions are normalized to -100% for Dy.

[b] Paramagnetic Fermi-contact contributions are normalized to 100% for Tb.

In the particular case (using a coordinate system associated with the principal axes of the magnetic susceptibility tensor), the expression for the pseudo-contact contribution to the LIS can be represented as it follows:

$$\delta_{PC} = \frac{10^{30}}{2N_A}\left[(\chi_{zz} - \overline{\chi})\left\langle \frac{3\cos^2\theta - 1}{r^3} \right\rangle + (\chi_{xx} - \chi_{yy})\left\langle \frac{\sin^2\theta\cos 2\phi}{r^3} \right\rangle\right] \quad (5)$$

Finally, if there is an axial symmetry of the complex, then equality $\chi_{xx}=\chi_{yy}$, together with formula (5) can be transformed to relationship (6):

$$\delta_{PC} = \frac{10^{30}}{3N_A}(\chi_{zz} - \chi_{xx})\left\langle \frac{3\cos^2\theta - 1}{r^3} \right\rangle \quad (6)$$

Based on these calculation methods, a majority of structural studies on lanthanide complexes in solutions have been carried out. The pseudo-contact contribution to the paramagnetic shifts for Ln cations in the ground state (with a definite value of J) has been calculated in Ref [39]. It has been assumed that the ground level is splittted in the ligand field into $(2J+1)$ sublevels (the splitting value being k_BT) taking into account that the electron spin–lattice relaxation time (T_{1e}) is much shorter than the correlation time of the rotational motion of the whole molecule ($_R$) (Table1) [7, 12]. In a series of isostructural lanthanide complexes one can to use the values of C_j and $<Sz>$ parameters (related to the δ_{PC} and δ_{FC} contribution to the LIS) for approximate NMR signals assignment.

Revealing the solution structure by paramagnetic lanthanide-induced shift analysis: common approaches

Many methods and techniques for LIS interpretation have been suggested and tested [41–44]. The development of these techniques has been conditioned by the researchers' intent of obtaining information concerning the spatial structure of Ln complexes (from the analysis of pseudocontact contributions to LIS). For the structural studies on lanthanide complexes two approaches of LIS analysis can be applied: a) with the use of an ab initio structural model and b) without any structural model.

For practical use, one can recommend the following efficient procedures for the analysis of LIS and relaxation rates.

(1) Separating pseudocontact and Fermi contact contributions to LIS via analyzing the ''lanthanide dependence of LIS'' [27–45] in some isostructural complexes.

This method has a number of variations:

(1A) A tabular qualitative description of the prevailing pseudocontact contribution to LIS via comparing the experimental normalized values of LIS based on the Bleaney constants for different Ln[39].

(1B) A quantitative analysis of a linear dependence of $(\delta_{obs}\text{-}\delta_D)/<S_Z>$ on $C_j/<S_Z>$ parameters (see Table 1) carried out according to Eq. (7) [39]:

$$\frac{\delta_{obs}-\delta_D}{\langle S_z\rangle}=F+G\frac{C_j}{\langle S_z\rangle} \tag{7}$$

The criterion of isostructural character for a series of complexes consists in the linearity of the dependence of $(\delta_{obs}\text{-}\delta_D)/<S_Z>$ on $C_j/<S_Z>$ in Eq. (7), where G and F parameters are represented by the constants in the series.

(1C) In addition to method (1B), there is also a LIS analysis method independent with respect to crystal field parameters *Cj* [7] based on Eq. (8).

$$\frac{\delta_{ij}^{para}}{\langle S_z\rangle_j}=\left(F_i-F_k\frac{G_i}{G_k}\right)+\frac{G_i}{G_k}\cdot\frac{\delta_{kj}^{para}}{\langle S_z\rangle_j} \tag{8}$$

where *i* and *k* indices correspond to *i*- and *k*- nuclei. All of these methods (from 1A to 1C) represent 'without structural models' techniques. The disadvantage of 'without structural models' methods consists in the fact that they are not very informative, since if the obtained dependences differ from linear ones, they are difficult to interpret even in a qualitative manner. Nevertheless, these methods have been successfully used to analyze the structural features in the series of homogeneous lanthanide complexes [7].

(2) Separating pseudocontact and Fermi contact shifts in a series of isostructural Ln complexes via measuring the ''Gd-induced shifts''.

This procedure is based on the fact that the pseudocontact shifts in Gd complexes amount to zero and hence one can estimate the F constant for the entire series of Ln complexes [39]. A significant broadening of NMR signals (owing to the relatively long value of T1e in the Gd cations), and high error values in chemical shift determination exhibit a disadvantage of the method.

(3) A least-squares fitting procedure is used to study the spatial structure of Ln complexes with branched ligands [42]. If a certain structural model is obtained (by the X-ray diffraction or quantum–mechanical modeling and other methods), one uses the analysis technique based on the optimization procedure of pseudo-contact contributions to the LIS, as shown in formulas (2–6) and (10) [40]:

$$AF=\left(\frac{\sum_{i,Ln}W_i(\delta_{LIS}-\delta_{calc})^2}{\sum_{i,Ln}W_i(\delta_{LIS})^2}\right)^{\frac{1}{2}}, \tag{9}$$

Here W_i is the weight factor equal to the reciprocal of the square of the determining LIS experimental error; *AF* is minimized parameter,δ_{LIS} is the experimental values of the paramagnetic chemical shifts (considering for the diamagnetic contributions); δ_{calc} is the optimized calculated values of pseudo-contact contributions to LIS. In the optimization procedures, the adjustable parameters are represented by the components of the magnetic susceptibility tensor in formulas (5) and (6), whereas the geometric parameters are given by constants. When Fermi-contact contributions can be neglected, this optimization method is satisfactory. Otherwise, several methods described above can be used to separate the pseudo-contact and Fermi-contact contributions to the LIS. Details and varieties of this method have been given [44]. In the general case, when analyzing Eq. (7), one can simultaneously use ^{1}H, ^{13}C, ^{19}F, ^{31}P etc. NMR data and data for different Ln ions, which depends on the system under study. The space of the fitting parameters can include both the spatial variables and the variables defining the pseudocontact and Fermi contact contributions to LIS for different Ln (then method 3 could be regarded as a variation of method 1). The number of independent fitting parameters could be reduced for lanthanide complexes having axial or effective axial symmetry (as a result of intramolecular motion) or for the nuclei for which the Fermi contact contribution could be neglected compared to the pseudocontact term [31, 32, 44, 45].

(4) A combined method for analyzing the structure of paramagnetic Ln complexes from LIS analysis and relaxation NMR spectroscopy data involves the following two techniques using the structural data obtained by analyzing the dipole lanthanide-induced enhancements of spin–lattice relaxation rates (LIR) (see the next section) [44]. This method has a few variations:

(4A) The relaxation enhancements are used to test the adequacy of the geometrical model applied in the LIS analysis.

(4B) The values of LIR used to reduce the number of unknown ''LIS analysis parameters'' (for example, by method 3). This method is applicable to both kinetically stable and unstable lanthanide complexes.

(5) A combined method for analyzing the structure of macromolecules (e.g., porphyrins, albumins,

oligonucleotides, proteins, DNA, etc.) based on their formation of complexes with paramagnetic lanthanide cations which combines LIS measurements with the complete ^{1}H NMR signal assignment (by 1D NOE technique as well as 2D NOESY, ROESY, TOCSY, and COSY experiments) [43].

(6) A combined method for the studies on the structure of complexes with paramagnetic *3d*- and *4f*-elements based on the studies on residual dipolar couplings (depending on magnetic field contribution to splitting $^{1}J_{NH}(B0)$). This has been applied to ^{15} N substituted proteins and DNA in D_2O solution using the results of 1D NOE, various 2D NMR techniques, relaxation NMR spectroscopy, paramagnetic shifts in NMR spectra [29, 41, 43–45] and computer molecular mechanics simulations and quantum chemistry calculations [51]. It should be noted that the use of the method requires NMR spectrometers with high magnetic fields (operating frequency > 600 MHz).

(7) A structure elucidation based on the studies on the Curie-spin contributions to the paramagnetic spin–spin relaxation rate enhancements (see the next section); this method is resently proposed [52]. The method requires NMR spectrometers with high magnetic fields (operating frequency > 500 MHz).

Lanthanide-induced paramagnetic relaxation rate enhancements

The modern theory of paramagnetic spin–lattice relaxation processes on the nuclei of ligand atoms in the complexes of paramagnetic lanthanides has been described in detail. [7, 12, 44, 53].The lanthanide-induced increase in spin–lattice relaxation rates on ligand nuclei in paramagnetic Ln complexes (with respect to the corresponding relaxation rates in isostructural diamagnetic complexes, for example, La or Lu) can be represented as (11) [54]:

$$R_1 = R_1^{(\mathrm{dip})} + R_1^{(\mathrm{cont})} + R_1^{(\mathrm{CS})}, \tag{10}$$

where R_1 is the increase in the spin–lattice relaxation rates; $R_1^{(\mathrm{dip})}$, $R_1^{(\mathrm{cont})}$, $R_1^{(\mathrm{CS})}$ are the dipole, contact, and Curie-spin contributions, respectively, in the spin–lattice relaxation rates.

The dipole contribution ($R_1^{(\mathrm{dip})}$) is caused by the intramolecular dipole–dipole interaction between the magnetic moments of the ligand nuclei (associated with spin *I*) and the magnetic moments of the electrons of the paramagnetic cation (associated with spin *S*). For lanthanide complexes, the contribution with a small value of the anisotropy of tensor *g* can be expressed by the following equalities (wherein the spin–lattice relaxation time of electrons $T_{1e} \ll 10^{-11}$ s):

$$R_1^{(dip)} = \frac{2J(J+1)\gamma_I^2 g^2 \mu_B^2}{15r^6}\left(\frac{3\tau_c}{1+\omega_I^2\tau_c^2} + \frac{7\tau_c}{1+\omega_s^2\tau_c^2}\right), \tag{11}$$

$$\frac{1}{\tau_c} = \frac{1}{\tau_e} + \frac{1}{\tau_R}, \tag{12}$$

Here, *J* is the value of the electron total angular magnetic moment; γ_I is the nuclear gyromagnetic ratio, *g* Lande factor of the electron; μ_B is the Bohr magneton, *r* is the distance between the nucleus *i* and the paramagnetic center; ω_I is the nuclear resonant frequency; ω_S electronic resonant frequency; τ_c is the characteristic correlation time; τ_e is the electronic relaxation time; τ_R is the correlation time of the rotational motion.

The second term in expression (11) can be represented according to the following equation:

$$R_1^{(cont)} = \frac{2}{3}\frac{J(J+1)(g-1)^2A^2}{\hbar^2}\left(\frac{\tau_e}{1+\omega_s^2\tau_e^2}\right). \tag{13}$$

Here *A* is the hyperfine interaction constant.

In most cases, the dipole contribution is dominant and the Fermi-contact contribution can be neglected, since it does not exceed the error in measuring the values of the relaxation rates. For example, the available estimated values of the dipole and contact contributions to the increase in the spin–lattice relaxation rates of protons are 10^2 s and 0.1 s^{-1}, respectively for lanthanide complexes with macrocyclic polyethers (MCPE) (assuming that the observed nucleus is proton or carbon, $r \sim 5$A, $T_{1e} \sim 10^{-13}$ c and $A \sim 10^6$ c^{-1}) [55].

As a result of the dipole interaction of nuclear spin with a local electronic magnetic moment arising, the Curie-spin contribution to increasing the rate of spin–lattice relaxation (R_1 (CS)) is realized (owing to the minimum difference in the splitting of electronic levels under the action of a magnetic field):

$$R_1^{(CS)} = \frac{2J^2(J+1)^2\gamma_I^4 g^4 \mu_B^4 H_0^2}{5r^6(3kT)^2}\left(\frac{3\tau_R}{1+\omega_I^2\tau_R^2}\right), \tag{14}$$

T: absolute temperature, H_0: magnetic field strength.

The Curie-spin contribution becomes comparable with the dipole contribution in magnitude in certain conditions (high magnetic field of the spectrometer, medium and high molecular mass of the complexes). In most cases, the Curie-spin contributions to the paramagnetic spin–lattice relaxation rate enhancements can be neglected.

Since both the dipole and the Curie-spin contributions to the increase in the spin–lattice relaxation of the nucleus *i* are proportional to the parameter r_i^{-6}, where r_i is the distance between the lanthanide cation and the resonating nucleus *i* (Fig. 1).

$$\frac{T_{1i}^{para}}{T_{1j}^{para}} = \left(\frac{r_i}{r_j}\right)^6, \tag{15}$$

Here T_{1i}^{para} and T_{1j}^{para} represent the time of paramagnetic spin–lattice relaxation for nuclei *i* and j, whereas r_i and r_j are the distances between the paramagnetic center (cation Ln^{3+}) and nuclei *i* and *j*, respectively. Most structural studies on lanthanide complexes based on paramagnetic spin–lattice relaxation (as shown in Eq. (15)) [56, 57]. As for spin–spin relaxation, there are some features that should be taken into account. The half-width of the signal is generally associated with the spin–spin relaxation time T_2 ratio:

$$W = 1/(\pi T_2) = R_2/\pi, \tag{16}$$

where *W* is the half-width at half-maximum signal, T_2 is the effective spin–spin relaxation time, R_2 is the transverse relaxation rate of a NMR signal. The value of the spin–spin relaxation time (SSR) in the paramagnetic complexes of Ln can be represented as the sum of the diamagnetic $R_2^{(dia)}$ and the paramagnetic $R_2^{(para)}$ contributions. The latter one can be divided into three components such as the dipole–dipole component, the Fermi-contact component, and the Curie-spin component. Furthermore, the chemical exchange may contribute (in general case) to T_2 relaxation too. In this case, special techniques have been used to calculate the relaxation components (see, e.g., Refs. [58, 59]). It should be noted that the chemical exchange processes are off the scope of present paper. Thus, total rate of spin–spin relaxation R_2 for paramagnetic lanthanide complexes can be given by the following relationship:

$$R_2 = R_2^{(dia)} + R_2^{(dip)} + R_2^{(FC)} + R_2^{(CS)}, \tag{17}$$

where R_2 is the rate of the spin–spin relaxation, $R_2^{(dia)}$ is the diamagnetic, $R_2^{(dip)}$ is the dipole, $R_2^{(CS)}$ is the Curie-spin, and $R_2^{(FC)}$ is the Fermi contact contribution to the transverse relaxation rate enhancement.

The diamagnetic contribution $R_2^{(dia)}$ could be considered using the studies on diamagnetic complexes of La or Lu [58–60]. Typically, the value of this contribution is from a few tenths to a unit of Hz.

The Fermi contact contribution to the transverse relaxation rate ($R_2^{(FC)}$) can be represented by the following relationship:

$$R_2^{(FC)} = \frac{J(J+1)}{3}\left(\frac{A_i}{\hbar}\right)^2\left(2\tau_{s1} + \frac{\tau_{s2}}{1+\omega_S^2\tau_{s2}^2}\right) \tag{18}$$

where *J* is the value of the total angular electron magnetic moment, A_i is the hyperfine interaction constant, $\hbar$—Planck's constant, τ_{s1} and τ_{s2} are the longitudinal and transverse electronic relaxation times respectively, ω_S is the electronic resonance frequency. The Fermi-contact is caused by the interaction via chemical bonds, and it is the most important for the nuclei located close to the Ln cation.

It is known that the dipole–dipole contribution ($R_2^{(dip)}$) significantly decreases with increasing distance between the resonating nucleus and the Ln cation:

$$R_{2i}^{(dip)} = \frac{4}{3}\left(\frac{\mu_0}{4\pi}\right)^2\frac{\gamma_I^2 g_J^2\beta^2 J(J+1)}{r_i^6}\tau_e \tag{19}$$

where μ_0 is the magnetic permeability of vacuum, g_J is Lande factor of the electron, γ_I is the nuclear gyromagnetic ratio, β is Bohr magneton, r_i is the distance between the nucleus *i* and the paramagnetic center, τ_e is the electron relaxation time.

The Curie-spin contribution also has a dipole nature and owing to the interaction of the nuclear spin with the local electron magnetic moment arising because of the minimal difference between the populations in the splitting of the electron levels under the influence of the magnetic field:

$$R_2^{(CS)} = \frac{1}{5}\left(\frac{\mu_0}{4\pi}\right)^2\frac{\omega_I^2 g_J^4\mu_B^4 J^2(J+1)^2}{r^6(3kT)^2}\left(4\tau_r + \frac{3\tau_r}{1+\omega^2\tau_r^2}\right) \tag{20}$$

where *k* is the Boltzmann constant, *T* is the absolute temperature, r_i is the distance between the nucleus *i* and the paramagnetic center, τ_r is the reorientational correlation time, ω_I is the nuclear resonance frequency. The Curie-spin contribution is determined by reorientational correlation time τ_r and has a strong temperature and field dependence. In some cases, the Curie spin contribution is comparable to the dipole–dipole one and can even be significantly predominant. The Curie-spin component is a quadratic function of the external magnetic field H_0 and the inverse temperature. Moreover, $R_2^{(CS)}$ also depends on the solution viscosity (as it is determined by a correlation time τ_r). In the particular case (under the condition of a strong magnetic field, medium viscous fluids, low or intermediate molecular weight complexes), the value of ω_I parameter significantly increases $\{(1+\omega_I^2\tau_r^2) >> 1\}$, and the expression for the Curie-spin contribution in formula (20) can be simplified as it follows:

$$R_2^{(CS)} = \frac{4}{5}\left(\frac{\mu_0}{4\pi}\right)^2\frac{\omega_I^2 g_J^4\mu_B^4 J^2(J+1)^2}{r^6(3kT)^2}\tau_r \tag{21}$$

The correlation time τ_r can be estimated using the Stokes–Einstein relation:

$$\tau_r = \frac{\eta M}{\rho N_A kT}, \tag{22}$$

where η is the dynamic viscosity of the solvent, *M* is molecular weight substances, ρ is density of the solvent, N_A is the Avogadro constant. The value of τ_r (for non-viscous aqueous

solutions and/or small molecules) is in the range from 10^{-9} to 10^{-11} s.

Thus, the total paramagnetic lanthanide-induced contribution to the relaxation rate enhancement is the sum of the dipole–dipole, the Fermi-contact and the Curie-spin components:

$$R_2^{(para)} = R_2^{(dip)} + R_2^{(FC)} + R_2^{(CS)} \quad (23)$$

It is assumed Fermi-contact component of the relaxation rate is weakly dependent on temperature. The dipole–dipole component decrease weakly in the temperature range from 273 to 330 K, whereas the Curie spin contribution rapidly decreases with temperature increasing.

A few words should be said here concerning the state of experimental observations of Curie-spin relaxation in complexes of Ln with PAPC and some other ligands. Currently, complexes of Dy^{3+} with DOTA, DTPA and DOTAM chelate ligands are considered in the literature as promising T_2-contrast agents for MRI. In the future these complexes could become more efficient relaxants even than Gd^{3+} complexes widely used in the high field MRI owing to the significant contribution of Curie-spin relaxation [61–63]. One of the crucial problems of the studies on paramagnetic relaxation processes of various paramagnetic lanthanide complexes is a search for the experimental conditions under which it is possible to separate a particular contribution of different types of electron-nucleus interaction to the relaxation rate. Relatively little number of publications are available in the literature on the Curie-spin contribution to paramagnetic transverse relaxation rate enhancement (CS-PTRRE) [64]. In particular, only a few examples of experimental studies on the field dependence of this contribution have been found in the case of Dy derivatives [59, 62–64]. In those works, the optimal conditions for obtaining the maximum of r_2 relaxivity (depending on the field and lifetime of water molecules in the first coordination sphere of Ln cations) have been found. However, the researchers neither have specifically discriminated the CS contributioN,Nor have examined its temperature dependence. In the recent work proposed [52]., an attempt has been made to take into account the CS-PTRRE experimentally. However, the studies have been carried out at low fields, and the calculated values of the CS contribution have shown to be only slightly greater than the determination error for relaxation rate. The pseudo-contact contribution has been found to prevail. To the best of our knowledge, the detailed investigations of CS-PTRRE for several lanthanides also have been carried [52, 65–68].

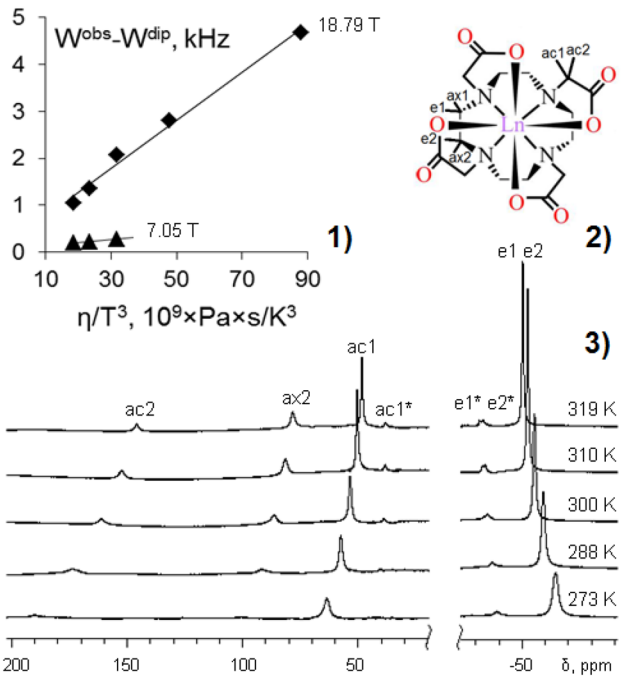

Fig. 2 Dependence of the difference of (W^{obs}—W^{dip}) on the parameter $\eta/T^3$and magnetic field for the ac2 protons of $[Ho^{3+}(DOTA)]^-$ in D_2O at 18.79 and 7.05 T (**1**); the molecular structure of $[Ln^{3+}(DOTA)]^-$ compounds (**2**); 800 MHz ^1H NMR spectra of $[Ho^{3+}(DOTA)]^-$ in D_2O at different temperatures (at 18.79 T), concentration of the complex 2×10^{-2} M and pH 7.0 (**3**); here Ln = Ho and Lu [65]

Revealing the conformation dynamics using dynamic NMR (DNMR)

Earlier [69], the molecular structure and temperature dependence of lanthanide-induced shifts (LIS) and conformational dynamics of $[Ln^{3+}(DOTA)]^-$ compounds, where Ln = Ho and Lu, have been studied using ^1H NMR in D_2O solution. The conformational dynamics has been caused by the interconversion of square-anti-prismatic (SAP) and twisted-square-anti-prismatic (TSAP) conformers [70, 71]. It has been supposed that the CS makes a considerable contribution to the paramagnetic relaxation rate in the case of compound $[Ho^{3+}(DOTA)]^-$, and this should be taken into account when studying the processes of chemical exchange in lanthanide complexes. Further, using the Ho complex with DOTA as an example, the studying the temperature dependence of CS contribution to the relaxation rate has been conducted [65]. This is the first example of the detailed studies on the temperature dependence of Curie-spin contribution to the paramagnetic transverse relaxation rate enhancements in lanthanide complexes other than dysprosium, taking into account the magnetic field strength and change of viscosity with temperature (Fig. 2). Thanks to this approach, the separation of the paramagnetic contributions (Curie-spin and dipole–dipole) has been achieved and it turned out that at

high magnetic fields (about 18 T), the Curie-spin contribution is predominant.

It should be noted that both the dipole and the Curie-spin contributions to the increase in the spin–spin relaxation of the nucleus i are also proportional to parameter r_i^{-6} (where r_i is the distance between the lanthanide cation and the resonating nucleus i) analogically to expression (15). Taking into account the increased role of Curie-spin contribution, this circumstance could be used to study the structure of lanthanide complexes (for example, in the case of a low relevance of longitudinal relaxation data for complexes of heavy lanthanides).

Thus, the use of the dynamic NMR (DNMR) to analysis the intramolecular dynamics of Ln complexes has its own peculiarities related to the paramagnetic properties of the complexes. The waveform is determined by parameters of chemical shifts and the half-width of the signals (for different positions) in the absence of exchange. When analyzing paramagnetic Ln complexes, it is necessary to consider the LIS dependence on temperature. In practice, it is performed by extrapolating the analytical dependence of LIS on temperature, to found the slow exchange region to the temperature range of intermediate and rapid exchange area. By analyzing the temperature dependence of the values of the exchange rate constants, one can obtain the energy characteristics of the process (free Gibbs energy ($\Delta G^{\neq}$), enthalpy ($\Delta H^{\neq}$) and activation entropy ($\Delta S^{\neq}$)). Hence, one can use the least-squares optimization procedure for the linear dependence of ln(k/T) on 1/T [72]:

$$\ln\left(k/T\right) = -\mathrm{DH}^{\neq}/RT + \mathrm{D}S^{\neq}/R + \ln\left(k_b/h\right), \tag{24}$$

k: reaction rate constant; R: gas constant; k_b: Boltzmann constant; h: Planck constant.

It is recommended that the study should be carried out at the maximum possible temperature range, and the greatest density of study points should be at the ends of the temperature range to reduce the errors of $\Delta G^{\neq}$, $\Delta H^{\neq}$ and $\Delta S^{\neq}$ [72].

With reference to the paramagnetic Ln complexes, it is possible to use the NMR to investigate the intramolecular dynamics of lanthanide complexes, [8] the ligand exchange kinetics and kinetics of complex formation; also one could to study the conformational lability of non-associated substrate molecules based on LIS of substrate molecules [72].

Another feature of DNMR application to the study paramagnetic Ln complexes consists in the fact that the range of measured rate constants is significantly broadened compared to a similar range in diamagnetic compounds. For example, to estimate the maximum of measured rate constant (k_{max}) for chemical exchange processes associated with conformational dynamics we use Ln complexes with cyclic polyethers [8]. According to Pitt-Anderson formula [72] to estimate the approximate of O-CH_2 in diamagnetic compounds has been $k_{max} \sim 10^6$ s^{-1}, while for paramagnetic compounds the corresponding value turned out to be $k_{max} \sim 10^{10}$ s^{-1}. This means that in the paramagnetic Ln complexes the range of the chemical exchange rates available for measurement can be significantly broadened compared to the range of rate constants in related diamagnetic compounds.

LIS in the NMR spectra of paramagnetic lanthanide complexes depending on temperature

The temperature dependence of LIS has been reported by B. Bleaney [39], and theoretically substantiated that LIS in the solutions of paramagnetic lanthanide compounds can be expanded in a series in powers of the inverse temperature, with the predominant contribution to T^{-2} dependence. In fact, the experimental studies confirmed did not have this dependence [73–76] shown that the temperature dependence of the LIS is empirically well described by a linear approximation from the inverse temperature T^{-1} [39]. Note that, the temperature dependence of the stability constant of these compounds has been not always correctly taken into account, since the studies have been carried out on kinetically unstable compounds. In the expansion of the LIS into a series in powers of the inverse temperature, the contribution of terms with high degrees (T^{-3}, T^{-4}, etc.) is almost always significant. In this case, the experimental paramagnetic chemical shift are well described by a linear dependence on the inverse temperature [31]:

$$\delta_{\mathrm{LIS}} = \mathrm{a} + \mathrm{b}/T, \tag{25}$$

Measurement temperature and construct a three-dimensional temperature distribution in animate and inanimate objects by using non-invasive radio-spectroscopic methods (NMR, MRI, EPR) have great prospects in medicine, biology, and modeling of physical and chemical processes. Based on chemical shift temperature dependence, temperature measurements have been performed on 2D and 3D of macro objects in vitro and in vivo by using NMR and MRI methods [77–80]. The basic methods for determining the temperature of biological objects are based on the temperature dependence of the chemical shift of protons of tissue water or the longitudinal relaxation time T_1 (with a sensitivity of about 0.01 ppm/K). Both of methods are used and validated in practice [81], but not enough for accurate temperature measurements in biological objects (usually ± 1 K). Paramagnetic LIS are more sensitive to temperature changes, therefore, it possible to measure the temperature with greater accuracy by using paramagnetic lanthanide complexes [82]. Based on this point, the attempts to use the temperature dependence of LIS in certain Tm^{3+} complexes with PAPC

and similar ligands (DOTA, DOTMA, DOTP) have been reported by using expression (18) or similar [83–86]:

$$\delta^{obs} = m \times t + n, \tag{26}$$

δ^{obs}: experimental paramagnetic chemical shift; t: temperature (°C); m: slope of the graph of δ^{obs} versus t; n: constant.

The temperature sensitivity of the paramagnetic chemical shifts $d(\Delta\delta_{ex})/dT$ can be defined as the modulus of the ratio of the difference in chemical shift values at temperatures T_1 and T_2 to the difference in these temperatures [69]:

$$d(\Delta\delta_{exp})/dT \approx \left|\frac{\delta(T_2) - \delta(T_1)}{T_2 - T_1}\right|, \tag{27}$$

where T_2 and T_1 are represented by the upper and lower boundary values of the temperature range, $\delta(T_2)$ and $\delta(T_1)$ are represented by the paramagnetic chemical shifts at temperatures T_2 and T_1, respectively.

In our opinion, the temperature sensitivity of chemical shift is one of the key parameters to characterize the accuracy of temperature determination by means of LIS analysis. The temperature sensitivity of the chemical shifts is of the order of 0.01 ppm/K in the most of diamagnetic compounds, however, it can achive relatively large values for paramagnetic compounds (up to 1.0 ppm/K) [83–86].

Currently, lanthanide complexes with PAPC ligands have been studied as thermo-sensitive sensors in single, relatively successful in vivo MRI experiments [87]. However, a relatively high error in the experimental temperature measurements has been observed, on the average higher than 0.5 K [81–85]. This could be caused by the application of a method for determining the temperature in vitro and in vivo, [87] as well as by a low sensitivity of devices and imperfections of MRI techniques. It is expected that further improvement in MRI-technology should make it possible to use these temperature effects for diagnostic purposes.

However, alongside with temperature, other factors such as thermodynamic equilibria, pH, ionic strength, etc. can also affect the paramagnetic chemical shift of the signal in vivo MRI experiments. However, the relationship between the temperature dependence of experimental paramagnetic chemical shift and other factors has not been almost studied. Previous, the studies on the temperature dependence of LIS about Ln complexes has been carried out mainly on in organic media [8–10]. To the best of our knowledge, there is only few investigations of the temperature dependences of Ln complexes on LIS in aqueous media, which except for single studies on lanthanide complexes based on PAPC ligands [81–85, 87] At present, empirical data on the temperature dependences of the LIS are mainly based on examples of relatively simple Ln complexes with PAPC ligands (with an attempt to relate this to pH, ionic strength, etc.). Hence, taking into account the pH change in solutions, it is of interest to study the temperature dependences of paramagnetic chemical shift for various lanthanides compounds with PAPC ligands (such as EDTA, DTPA, DOTA, etc.) to solve the general problem of determining the parameters of chemical exchange.

In the following sections of this review, we show the examples of studying molecular dynamics taking into account the temperature dependence of paramagnetic chemical shift and the effect of pH in aqueous solutions.

Table 2 The stability constants lgK_{ML} and the energy parameters of complexation (enthalpy ΔH and entropy ΔS) for Ln^{3+} with EDTA complexes [89]

Ln^{3+}	lgK_{ML}	ΔH, kJ/mol	ΔS, kJ/mol
La^{3+}	15.5	− 12.1	255
Ce^{3+}	16.0	− 12.1	264
Pr^{3+}	16.4	− 13.4	268
Nd^{3+}	16.6	− 15.1	268
Sm^{3+}	17.1	− 14.2	281
Eu^{3+}	17.4	− 10.9	297
Gd^{3+}	17.4	− 7.1	310
Tb^{3+}	17.9	− 4.6	327
Dy^{3+}	18.3	− 5.0	335
Ho^{3+}	18.6	− 5.9	335
Er^{3+}	18.9	− 7.1	335
Tm^{3+}	19.3	− 8.0	343
Yb^{3+}	19.5	− 9.6	340
Lu^{3+}	19.8	− 10.5	343

Paramagnetic lanthanide complexes with PAPC ligands

Lanthanide complexes with EDTA

We can mention that the EDTA-ligand is used to treat heavy metal poisoning in medicine [88], in food and pharmaceutical industry, and micronutrient complexes in mineral fertilizers [89] and also used in steam boilers and heating systems. In analytical chemistry, EDTA is used primarily as masking reagent for complexometric titration, and widely for biochemical studies.

EDTA with lanthanides formed strong complexes with 1:1 of stoichiometry, as shown in Table 2. The structure in the solid phase of complexes various of the metals such as rare-earth elements with EDTA has been reported in literature [90]. Various compositions of complexes are formed in different conditions, [89] for example: $[Ln_2(OH)_2(EDTA)]$ has been formed with an excess of the metal cation and at pH > 6, $[Ln_4(EDTA)_3]$ has been formed with at pH = 2–6, depending on the pH, [Ln(HEDTA)] has been formed

at pH = 2–3, and $[Ln(EDTA)_2]^{5-}$ with an excess of the ligand. In particular, monohydroxocomplexonate $[Ln(OH)(EDTA)]^{2-}$ has been formed with pH > 12, and normal complex $[Ln(H_2O)_n(EDTA)]^-$ complex has been formed in a wide pH range 3–12 at a metal–ligand ratio amounting to 1:1.

Typically, owing to the deficiency of factual material concerning the structure and molecular dynamics of complexes formed by the paramagnetic Ln and EDTA in solution, one can distinguish at least three main types of molecular dynamics that occur in the complexes of Ln with EDTA as it follows.

They are: firstly, the intermolecular kinetics of exchange between water molecules and paramagnetic cations that bind EDTA [91, 92]; secondly, the intermolecular dynamics associated with the coordination processes between the metal cation and the EDTA ligand; thirdly, the intramolecular dynamics of conformational isomerization of complexes. One example consists in the fact that the activation energy of intermolecular water exchange in related complexes has been found in the case of $[Fe(H_2O)(EDTA)]^{2-}$ complex ($\Delta G^{\neq}_{(298\,K)} = 38$ kJ/mol). [88] There have been made unsuccessful attempts to establish any correlations between the parameters of intermolecular dynamics (associated with water exchange) and intramolecular dynamics (associated with the processes of conformational isomerization), since the intramolecular dynamics could not be described with the use of NMR data obtained in these studies.

The first attempts to measure the rate constant of dissociation of $[Ln(H_2O)_n(EDTA)]^-$ complexes in aqueous solutions have been reported (Ln: La^{3+}, Lu^{3+}) [23, 24, 93]. Recently, ligand exchange processes for $[Ln(H_2O)_n(EDTA)]^-$ have been analyzed on the basis of ^1H NMR experiments (Ln: La^{3+}, Pr^{3+}, Eu^{3+}, Tb^{3+}, Ho^{3+}, Tm^{3+}, Yb^{3+} and Lu^{3+}) [94–99]. Proposed corresponding kinetic scheme for ligand exchange processes is presented at Fig. 3. Nevertheless, studying the pH effect on the processes of intermolecular dynamics in Ln complexes with PAPC ligands is still insufficient. The changes between pH and complex composition have been studied by only using Eu and EDTA complexes by NMR measurements [100, 101] And the processes of intramolecular dynamics associated with conformational isomerisation has been only reported the example of diamagnetic complexes [M(EDTA)] aq, (M: Sc^{3+}, Y^{3+} and La^{3+}) and paramagnetic complex $[Er(EDTA)]^-$ [92, 102].

Earlier for the complexes $[M(EDTA)]^{2-}$ and $[M(H_2O)(EDTA)]^{2-}$ (M: Fe^{2+} or Zn^{2+}) have been introduced a nomenclature of conformational isomers displayed in the form of codes [91]. These codes contain the symbols Δ-Λ that determine the overall chirality of the complex, such as the symbols δ_E-λ_E determine chirality with respect to the ethylenediamine fragment, and the symbols δδδδ-λλλλ determine chirality with respect to the iminodiacetate groups. It can be assumed that the scheme of designations of conformational isomers is also generally suitable for describing the structural-dynamic processes occurring in $[Ln(H_2O)_n(EDTA)]$ complexes [91]. Thus, according to NMR data for diamagnetic complexes of Sc^{3+}, Y^{3+} and La^{3+} with $EDTA^{4-}$ [92], only two structural isomers are observed in the system in place of the proposed six isomers. This

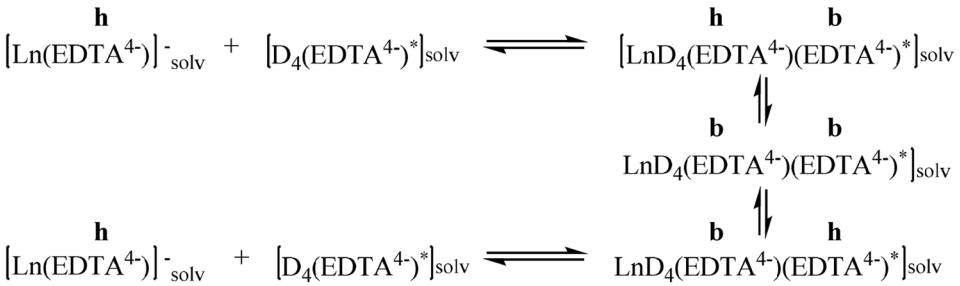

Fig. 3 The kinetics of ligand exchange for lanthanide complexes of the yttrium subgroup [98]. The "h" over the designations of the EDTA ligand mean a six-dentate ligand, "b" is a bidentate ligand. One of the exchanging ligands is marked with an asterisk "*"

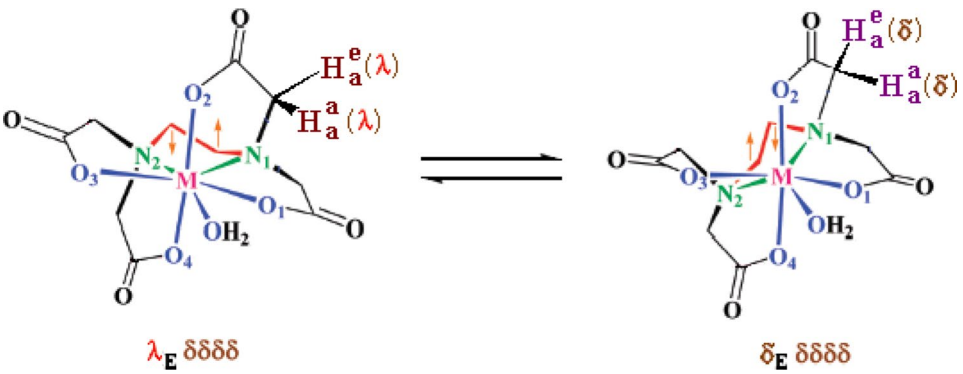

Fig. 4 Processes of intramolecular conformational dynamics in solutions of complexes $[Er(H_2O)_n(EDTA)]^-$. (Λ) and (λ) are respectively the equatorial and axial protons (δ) and (δ) of the acetate groups of the conformer $\Delta\lambda_E\delta\delta\delta\delta$ and $\Delta\delta_E\delta\delta\delta\delta$, respectively

Table 3 Activation parameters of intramolecular dynamics processes in metal complexes with EDTA

Metal ion	Cationic radius, Å	Activation energy, $\Delta E^{\neq}_{a}$ (kJ/mol)	Activation enthalpy, $\Delta H^{\neq}$ (kJ/mol)	Free activation energy of processes of intramolecular dynamics, $\Delta G^{\neq}_{298}$, (kJ/mol)	References
Sc^{3+}	0.89	69.5	67	–	[92]
Er^{3+}	1.03	–	–	50	[102]
Y^{3+}	1.04	42.0	39.6	–	[92]
La^{3+}	1.17	34.9	32.5	–	[92]

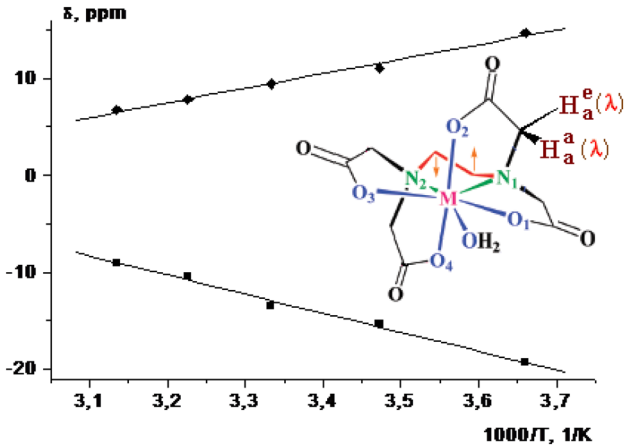

Fig. 5 Under fast exchange conditions the dependence of averaged paramagnetic LIS from 1/*T* in 800 MHz ^{1}H NMR spectra for protons $H_a^{\,e}$ (filled diamond) and $H_a^{\,q}$ (filled square) of the $[Er(H_2O)_n(EDTA)]$ complex; Solvent: D_2O [102]

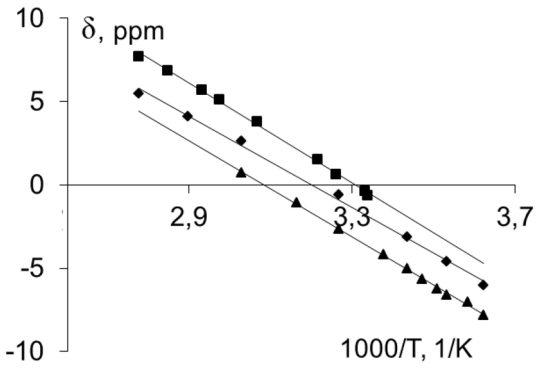

Fig. 6 Dependences of paramagnetic chemical shift on 1/*T* for the signal of hydrogen atoms of CH_2 groups of the ethylenediamine fragment in complex $[Yb(H_2O)_n(EDTA)]^-$ under different conditions: pH 0.7 (filled square), pH 1.1 (filled diamond), PH 7.5 (filled triangle) [104]

observation is corresponded with the work [102] where paramagnetic complex of Er^{3+} with $EDTA^{4-}$ has been studied. The relatively fast molecular dynamics associated with the chemical exchange of coordination water also can not determined by NMR methods. The processes of water exchange should significantly change the geometry of the complex, although did not have experimental confirmation [88].

In this part, the kinetics of the chemical exchange processes between $\Delta\lambda_E\delta\delta\delta\delta$ and $\Delta\delta_E\delta\delta\delta\delta$ conformers of the $[Er(H_2O)_n(EDTA)]$ complex in an aqueous medium has been presented, which is the first example of a detailed study the intramolecular dynamics of paramagnetic erbium complexes [103]. In the ^{1}H NMR spectra of the complex $[Er(H_2O)_n(EDTA)]$, the change in the shape of the signals of iminodiacetate protons by the chemical exchange is observed in aqueous solutions. Presumably, this exchange is caused by the processes of intramolecular conformational dynamics, as shown in Fig. 4. (the bidirectional vector "↔" denote chemical exchange processes).

The inversion of the central ethylenediamine fragment in the five-membered N–C-C-N-M cycle in $[Er(H_2O)_n(EDTA)]^-$ is accompanied by the exchange between the following protons: (λ) ↔ (δ) and (λ) ↔ (δ). According to the reported procedure [72], the calculated relative proportion for nuclei in pairs of exchanged signals (λ), (δ) are 0.7: 0.3 and (δ), (λ) are 0.7: 0.3, respectively, at ambient temperature.

Studying the temperature dependence of the rate constants of chemical exchange, have been obtained the Gibbs free energy of activation of the chemical exchange processes $\Delta G^{\neq}_{298} = 50 \pm 4$ kJ/mol. As shown in Table 3, the value of the free activation energy is comparable with the energy barriers of conformational transitions in EDTA complexes with diamagnetic metal cations [92]. In Table 3, it is shown that the value of the energy barrier increases monotonically with increasing ionic radius of the metal cation. Moreover, this effect is observed in a series of complexes $[M(EDTA)]^-$ with other metals (Ba^{3+}, Y^{3+}, La^{3+}). The analogous regularity is called "Lanthanid compression"effect" [7, 12].

The temperature dependences of paramagnetic LIS of $[Er(H_2O)_n(EDTA)]$ complex for protons of various groups are shown in Fig. 5. In 800 MHz ^{1}H NMR spectra, the experimentally obtained LIS dependences on the parameter 1/*T* of the paramagnetic LIS for protons $H_a^{\,e}$ (♦) and $H_a^{\,q}$ (■) of the $[Er(H_2O)_n(EDTA)]$ complex are linear [101]. The maximum temperature sensitivity of the LIS has been calculated for the protons of the CH_2 groups of the iminodiacetate

fragment of the $[Er(H_2O)_n(EDTA)]$ complex, and $d(\Delta\delta_{ex})/dT = 0.3$ ppm/K in temperature range from 320 to 370 K.

As shown in Fig. 6, the dependences of the paramagnetic chemical shift values on $1/T$ for the signals of the hydrogen atoms of the CH_2 groups of the ethylenediamine fragment in complex $[Yb(H_2O)_n(EDTA)]$ have been differ for various pH values, unlike the lanthanide complexes DTPA and DOTA [104].

It can be assumed that the change in the temperature dependence of paramagnetic chemical shift in dependence on pH owing to the interconversion of at least two forms of the complex and a fast reversible process of protonation of the complex.

Thus, research status of Ln with EDTA complex includes: (1) there are very few experimental studies on intramolecular dynamics associated with conformational isomerization of paramagnetic complexes of Ln with EDTA by using NMR; (2) at present, the processes of intermolecular kinetics of exchange between water molecules and paramagnetic cations that bind EDTA has rarely studied; (3) there has been few studied the pH effect to the processes of intermolecular dynamics in complexes of Ln with PAPC ligands; (4) separate the investigation of Ln complexes in aqueous solutions based on the temperature dependence of LIS have been reported.

Lanthanide complexes with DOTA-like ligands

Upon the recent burst in scientific research concerning magnetic resonance imaging (MRI), [7, 12] the lanthanide compounds and, in particular, the complexes of Gd^{3+} with macrocycles ligands have become some species among numerous paramagnetic contrast agents. In this part our studies have been focused on the $[Ln^{3+}(DOTA)]^-$ complexes and covered the solution dynamics of $[Ln(dota\text{-}like)(H_2O)]$ complexes. The conformational rigidity, high thermodynamic and kinetic stability exhibited by Ln^{3+} (DOTA) complexes are caused by a very good matching between the sizes of Ln^{3+} ions and the preformed cavity of the DOTA ligand. There are two main types of dynamic processes occurring in aqueous solutions of lanthanide complexes with DOTA ligands: (1) intramolecular dynamics caused by the interconversion of $[Ln(H_2O)_n(DOTA)]^-$ conformers; (2) exchange between coordinated water and cation Ln.

In solution, the coordinated water molecule involved in $[Ln(H_2O)_n(DOTA)]^-$ rapidly exchanges with the bulk solvent, and in the case of $[Gd(DOTA)]^-$, this leads to an overall, considerable increase in the relaxation rate of the solvent water protons [105]. These two properties are of primary importance in promoting the use of $[Gd(DOTA)]^-$ as a contrast agent for MRI applications [106, 107]. However, the questions concerning the structures of the aqueous solutions as well as the influence of some external factors [temperature, pH, presence of other potential rare-earth cation ligands (proteins)] on the gadolinium coordination sphere have not been resolved yet. We can mention as an example the local structures of $[Gd(DOTA)]^-$ complexes in the crystalline state (at a room and at a low temperature) and in aqueous solutions exhibiting various pH values at different temperatures reported by S. Benazeth et al. [107, 108]. They presented that from neutral pH to a value of 1.5, the local environment and complex dynamics around the gadolinium ions have been conserved up to 4.5 Å, and the structure agreed well with the known crystallographic data. On the other hand, the signals of X-ray absorption fine structure (XAFS) for $[Gd(DOTA)]^-$ complexes have exhibited

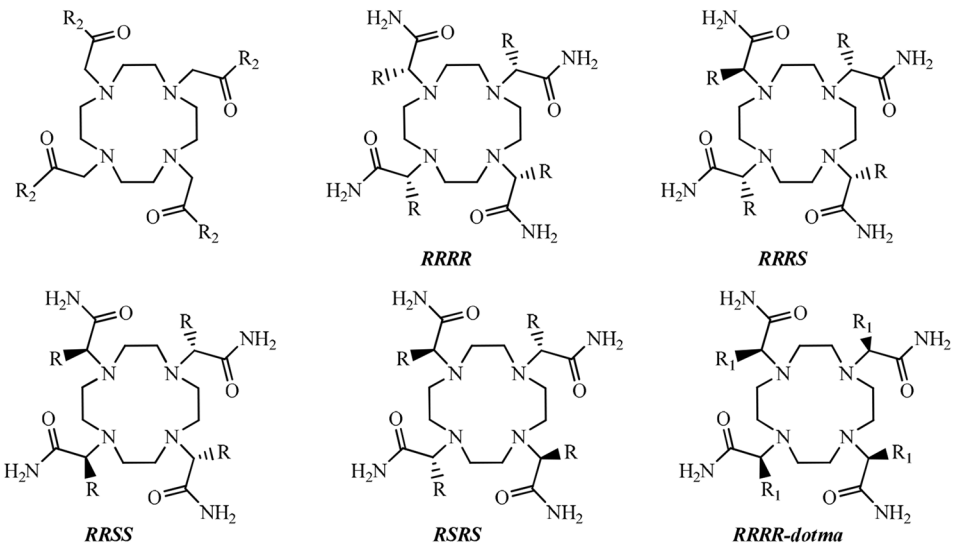

Fig. 7 Structures of the tetra (carboxyethyl) derivatives of DOTA. [107]

Fig. 8 Ditopic ligand of DOTA

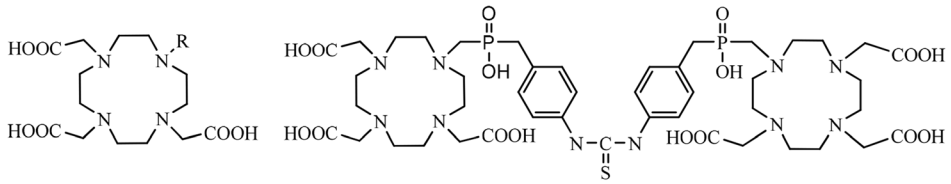

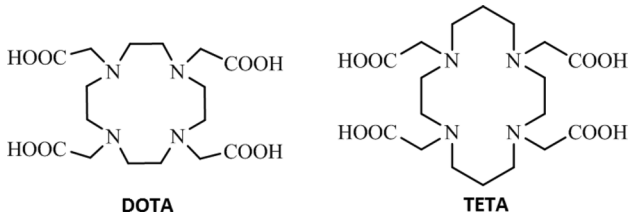

Fig. 9 The structural formulas of DOTA and TETA

only a slight dependence on pH. Meanwhile, no significant changes have been observed in the two different cases: crystalline state and aqueous solutions at pH 1.5–7. The slight changes with temperature are related to a small increase in the Debye–Waller (DW) factors.

There are scarce data concerning the energy parameters of intermolecular dynamics associated with water exchange. One of the examples consists in the exchange between the molecules of the coordination water in the $[Gd(H_2O)_n(DOTA)]^-$complex and water in the solution has been studied according to ^{1}H NMR spectroscopy and reported value of the free activation energy $\Delta G^{\neq}_{298} = 35$ kJ/mol for processes of water exchange [33, 109].

Woods et al. [33, 109–111] have studied the solution structure and the dynamics of metal-bound water exchange in a series of diastereoisomeric gadolinium complexes of tetra(carboxyethyl) derivatives of DOTA. They reported that the rate of water exchange in the gadolinium complex has been determined by ^{17}O NMR to be the fastest for the (RRRR) isomer [$\tau_m = 68$ ns (298 K)] to correlate very well with the fraction of the twisted square anti-prismatic isomer (as shown in Fig. 7).

A case involves a detailed NMR and relaxometric studies on lanthanide(III) complexes with novel "ditopic" ligand of general formula $[Ln_2(CS(DO3A\text{-}P^{NBn})_2)(H_2O)_2]^{2-}$ have been investigated by P. Hermann [112] (Ln = Y, Eu, Gd, Dy) (Fig. 8). By the measurement of the dysprosium(III)-induced the ^{17}O NMR shifts have determined the presence of one water molecule in the first coordination sphere. The structural and dynamic relaxivity-controlling parameters have been assessed by a simultaneous fitting of the variable temperature ^{17}O MR and ^{1}H NMRD relaxometric data. The mean water residence lifetime ($^{298}\tau_M$) has been found to be 53 ns, one of the shortest values reported for ditopic complexes. In this report, the two lanthanide(III) metal ions are nine-coordinate with one inner-sphere water molecule. In aqueous solution the complexes are present as a mixture of stereoisomers mutually interconverting at high temperature. The rate of exchange found is the highest measured for dinuclear Gd(III) complexes ($[Gd_2(CS(DO3A\text{-}P^{NBn})_2)(H_2O)_2]^{2-}$): $^{298}k_{ex} = (1.9 \pm 0.2) \times 10^7$ s^{-1}. Which is may owing to the presence of a sizeable contribution from water molecules hydrogen-bonded to the phosphinate groups and by a reorientational motion of the complex largely isotropic (As shown in Fig. 8).

It is interesting in studying the interrelationships between the structure, paramagnetic properties, and the molecular dynamics of Ln-DOTA complexes and DOTA-like ligands [60, 109, 110, 112–120]. The example of first type about intramolecular dynamics in DOTA and DOTA complexes with La^{3+}, Eu^{3+}, Yb^{3+} and Lu^{3+} have been reported based on using 2D EXSY NMR techniques and determining the coalescence temperature [119]. The molecular mechanics and dynamics calculations, kinetics, and laser-excited luminescence of trivalent lanthanide complexes of macrocyclic polyaminopolycarboxylate ligands TETA and DOTA have been studied by C. A. Chang groups [121]. The calculated bond distances and overall structures of $[Ln(DOTA)]^-$and Ln(TETA)-have been in agreement with the single-crystal and solution NMR structural data. They also used a stopped-flow spectrophotometric method to study the formation kinetics of the aqueous Ce^{3+}-TETA/DOTA systems in the pH range 6.1–6.7 (Fig. 9). Kinetic studies revealed that the formation rates of the Ce(TETA) -complex are smaller at lower pH and temperature but become greater at higher pH and temperature, as compared to those of the Ce(DOTA)-complex. This is attributed to the lanthanide ion and both mono- and di-hydroxide ion assisted TETA conformational reorganization and higher kinetic activation parameters. The presence of a di-hydroxide ion assisted intermediate rearrangement pathway could make the Ce(TETA)-complex formation rate faster at higher pH, and the higher activation barrier makes Ce(TETA)-complex formation rate slower at lower pH, as compared to those of the Ce(DOTA)-complex.

Eu^{3+} as the neighbour of Gd^{3+} is often used for study structural and dynamics in solutions. The bound water

signal could be observed by NMR at low temperature in a mixture of water and CD_3CN on the positively charged Eu^{3+} complex of DOTAM, the tetraamide derivative of DOTA, as a consequence of a very slow water exchange rate [122]. Lately, ^{1}H NMR line-shape analysis and magnetisation-transfer experiments at variable temperature and pressure have been used to elucidate the solution dynamics of both *M* and *m* isomers of three [Eu(dota-tetraamide)(H_2O)] complexes (DOTMAM, DTMA and DOTAM) [70, 71] (As shown in Fig. 10). The method directly observates the bound water signal of ^{1}H NMR and allows the water-exchange rates on each isomer to be measured individually. They are definitely independent of the ligand for both *M* and *m* isomers (*M*: $k^{298}_{ex} = 9.4 \pm 0.2 \times 10^3\ s^{-1}$

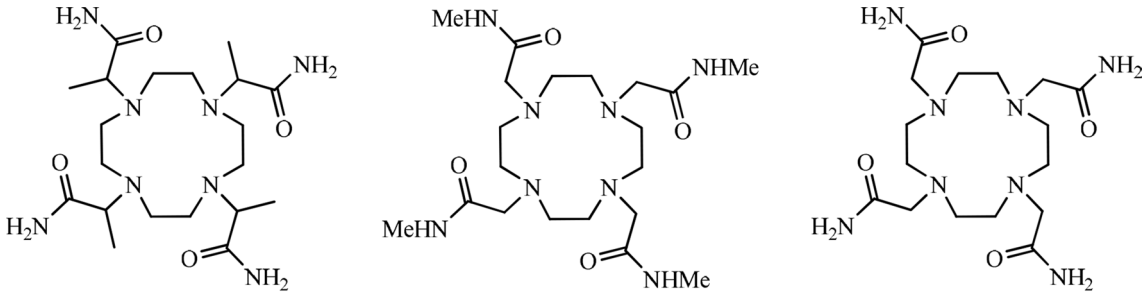

Fig. 10 Structural formulas of DOTA and DOTA derivatives

Fig. 11 Structures of the Pyridine-N-Oxide Analogues of DOTA Ligands

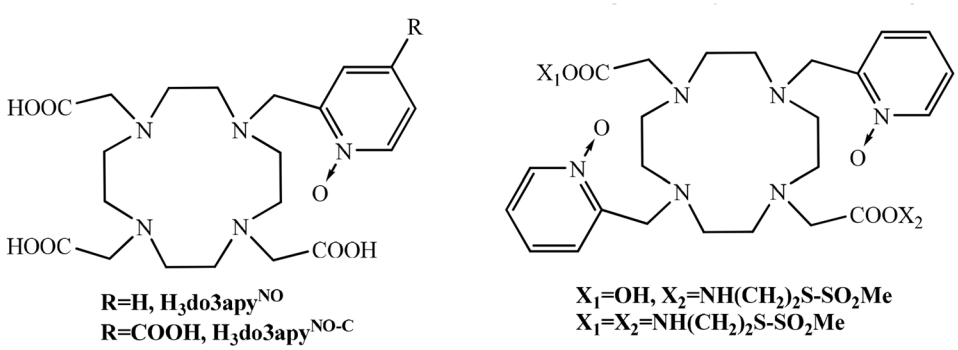

Fig. 12 DOTA-tetraamide ligands having side-chain arms

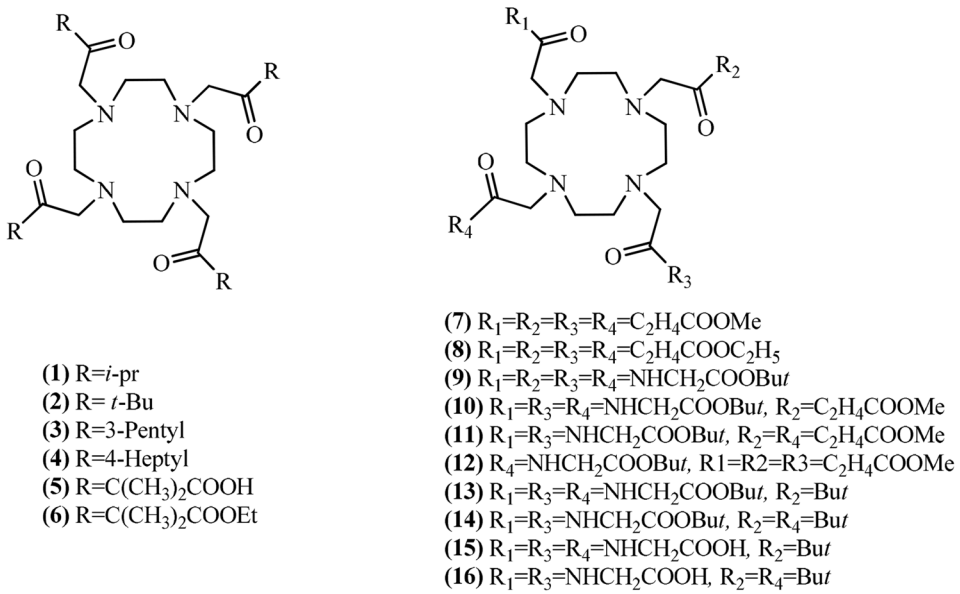

for $[Eu(dotam)(H_2O)]^{3+}$, $8.2 \pm 0.2 \times 10^3$ s^{-1} for Eu(dtma) $(H_2O)]^{3+}$ and $11.2 \pm 1.4 \times 10^3$ s^{-1} for $[Eu(dotmam)^{-}(H_2O)]^{3+}$; *m*: $k^{298}_{ex} = 474 \pm 130 \times 10^3$ s^{-1} for $[Eu(dotam)(H_2O)]^{3+}$, $357 \pm 92 \times 10^3$ s^{-1} for $[Eu(dtma)(H_2O)]^{3+}$, and proceed through a dissociative mechanism (*M* isomers: $\Delta V \geq +4.9$ cm^3mol^{-1} for $[Eu(dotam)(H_2O)]^{3+}$ and $\Delta V \geq +6.9$ cm^3mol^{-1} for $[Eu(dtma)(H_2O)]^{3+}$.

The replacement of one of the acetate pendant arms with a 2-methylpyridine-N-oxide group in the molecule of DOTA to alter the coordination properties of the ligand in Ln^{3+} complexes, and the structural properties of the complexes both in solution and in the solid state have been investigated by P. Hermann (As shown in Fig. 11) [123]. For the first time in the Ln^{3+} complexes of DOTA-like ligands have been observed parallel (syn-SA) or opposite (anti-SA) orientations the pyridine ring relative to the rotation of the coordinated acetate arms. The variable-temperature ^1H NMR spectra of Nd^{3+}, Eu^{3+}, and Yb^{3+} complexes show that the twisted-square-antiprismatic (TSA) isomer is strongly destabilized and the complexes exist mostly as the square-antiprismatic (SA) isomers (98% for Eu^{3+} at -35 °C). The exchange between the TSA and SA isomers is fast at room temperature compared to that of the NMR time scale.

Sherry reported six novel DOTA-tetraamide ligands having side-chain amide arms with varying hydrophobicity and polarity, and a series of novel DOTA-derivatives having a combination of amide and ketone donor groups as side-arms (Fig. 12) [124, 125]. The water exchange observed on the chemical shift of the Eu^{3+}-bound water resonance, have been investigated by means of high resolution NMR spectroscopy.

The results show that introduction of steric bulk into the amide side-chain arms of the europium(III) complexes not only favors formation of the mono-capped twisted square antiprism (TSAP) coordination isomers, the isomer that is generally less favourable for chemical exchange saturation transfer (CEST), but also accelerates water exchange in the mono-capped square antiprism (SAP) isomers. However, converting single methyl groups on these bulky arms to carboxyl or carboxyl ethyl esters results in a rather dramatic decrease in water exchange rates, about 50-fold. Thus, steric bulk, polarity, hydrophobicity of the amide side-chains, each contribute to organization of water molecules in the second hydration sphere of the europium(III) ion and this in turn controls water exchange in these complexes. The results also show that the bound water residence lifetimes (τ_m) have been found to vary dramatically with the chemical structure of the side-arms.

Although an estimation of the isomeric ratio of $[Ln(DOTA)]^-$ complexes has already been reported [70, 126], in the case of $[Pr(DOTA)]^-$ and $[Lu(DOTA)]^-$ it has been not possible to evaluate the actual isomer ratio by peak integration at 298 K, because the isomers are not in slow exchange on the NMR timescale at this temperature. For all

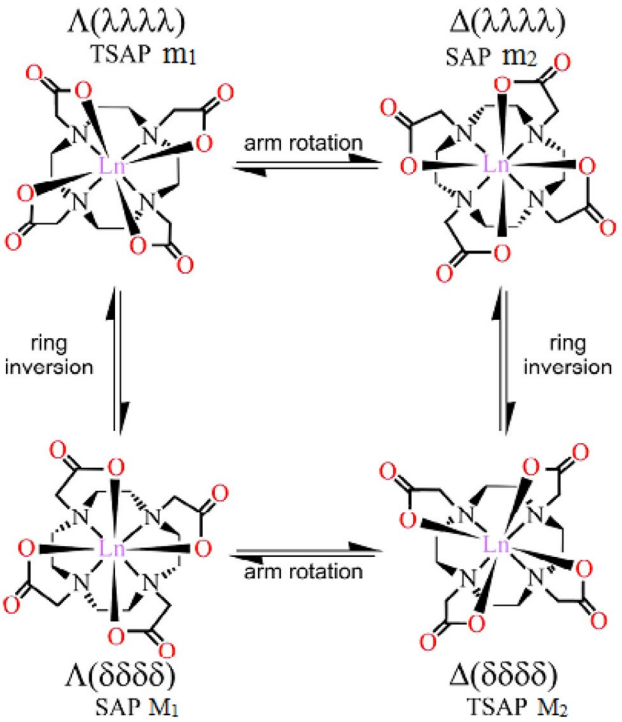

Fig. 13 Schematic representation of the structure and dynamics of the diastereoisomers of the Ln(DOTA)-complexes. The symbols Λ and Δ refer to the helicity of the acetate arms, and λλλλ and δδδδ, to the cycle. Here the conformational process is shown for the *M* and *m* forms but is equally applicable to *M*′and *m*. M_1 and M_2, as well as m_1 and m_2 named in agreement with the literature [70, 119] are NMR indistinguishable enantiomeric pairs respectively for the *M* and *m* forms detected by NMR

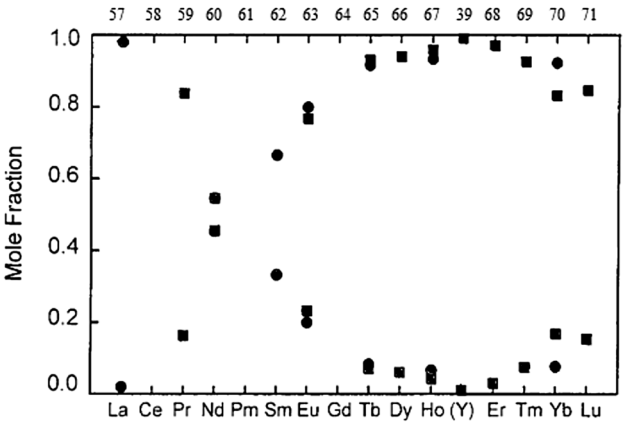

Fig. 14 Molar fractions of the isomers m (open symbols), m′(barred symbols), and M (filled symbols) of $[Ln(DOTA)(H2O)_x]^-$ as a function of the complexed metal ion from 1H-NMR spectroscopy (0.15 M $[Ln(DOTA)]^-$, pH = 7.0, T = 298 K, ionic strength = 0.3 M): (■) [60, 70, 127], (filled circle) [126]

the paramagnetic $[Ln(DOTA)]^-$ complexes for which two isomers could be observed by ^{1}H-NMR spectroscopy, one has been found to have larger paramagnetic shifts (larger susceptibility anisotropy) than the other. Both in solution and in the crystalline phase, the Ln-DOTA complexes exist as a pair of conformational isomers, referred to as *M* (square antiprismatic) and *m* (twisted square antiprismatic), differing in the orientation of the planes, the first one is formed by the N-atoms of the macrocycle, and four O atoms of iminoacetate groups. The angle between these planes is 40° and 24° for SAP (sometimes abbreviated as *M*-isomer) and TSAP (*m*-isomer), respectively. Figure 13 shows a schematic representation of the structure and dynamics of the diastereoisomers of the $[Ln(DOTA)]^-$ complexes. Two isomers are actually observed in solution in the ^{1}H- and^{13}C-NMR spectra of all $[Ln(DOTA)]^-$ complexes in slow exchange at room temperature, one with larger shifts (owing to larger anisotropic susceptibility) than the other.

For complexes $[Ln(H_2O)_n(DOTA)]^-$ (n = 0, 1, 2), the relative populations of conformers depends on the type of Ln [60]. Inspection of the ^{1}H- and ^{13}C-NMR spectra along the lanthanide series suggested that an inversion in *M* and *m* populations occurs in a number of lanthanide cations (starting with lanthanum and ending with lutetium) [60, 70, 127] (Fig. 14).

The rate constants for the dynamic processes of the interconversion of the conformational isomers of *M* and *m* are in the range of 10 to 200 s^{-1}. Whereas in $[Nd(DOTA)]^-$ the two isomers appear almost equimolar, for the lighter La, Ce, and Pr one isomer (likely the *m* isomer) is more abundant. Conversely, for the heavier ions it could be concluded that the main species has the structure of the *M* isomer. As opposed to all of the other paramagnetic ions, wherein the *M* isomer has the larger susceptibility anisotropy, in the Tm^{3+} chelate the more intense, less shifted proton signals are assigned to the *M* isomer [126], so that the isomer fractions for Tm^{3+} fit into the continuous variation from Er^{3+} to Yb^{3+} (see Fig. 14). For the lanthanides heavier than Ho^{3+}, the mole fraction of *M* decreases again with decreasing ionic radius. And for most of the DOTA and lanthanides complexes the free energy of activation of the exchange processes between the conformers is range from 50 to 65 kJ/mol (Table 4) [60, 70, 71, 126]. The free activation energy $\Delta G^{\neq}_{298}$ of a series of $[Ln(H_2O)_n(DOTA)]^-$ complexes increases from La to Yb, could be owing to the decrease of ionic radius with an increase in the atomic number Ln («lanthanide contraction») [8]. The experimentally values of the rate constants, activation parameters of the processes of conformational isomerization and ligands exchange with EDTA and DOTA ligands for Ln with PAPC complexes are significance to synthetic chemists for isolating conformational isomers in related compounds.

Table 5 The enthalpy ΔH^o and the entropy ΔS of the equilibrium isomerization processes SAP↔TSAP of the complexes $[Ln(H_2O)_n(DOTA)]^-$ (Ln = Ho, Er, Tm, Yb, Lu)

Ln	K^{298}	ΔH^o, kJ/mol	ΔS^o, J/mol × K	References
Ho	0.04 ± 0.01	20 ± 1.1	39 ± 5	[69]
Er	0.03	–	–	[60]
Tm	0.08	16.2 ± 0.9	33 ± 3	[60]
Yb	0.20	17.5 ± 0.7	45 ± 2	[60]
Lu	0.18	10.1 ± 0.1	18 ± 1	[60]

Table 4 Activation free energies ($\Delta G^{\neq}_{298}$, kJ mol^{-1}), derivative of experimental lanthanide-induced shifts ($d(\Delta\delta ex)/dT$, ppm/K) for different types of conformational molecular dynamics (SAP-TSAP, TSAP-SAP or enantiomerization), and methods used for the investigation of intramolecular dynamics in Ln^{3+} complexes with DOTA derivatives

Ln^{3+} cation	Ionic radius, Å	$\Delta G^{\neq}_{298}$, kJ/mol SAP-to-TSAP	$\Delta G^{\neq}_{298}$, kJ/mol TSAP-to-SAP	$\Delta G^{\neq}_{298}$, kJ/mol Enantio-merization	Method	$d(\Delta\delta_{ex})/dT$, ppm/K	References
$[La(H_2O)_n(DOTA)]^-$	1.17	–	–	60.7 ± 1.2	^{1}H and ^{13}C BSA$^{\#}$	0.0$^{\&}$(^{1}H)	[128, 132]
$[Pr(H_2O)_n(DOTA)]^-$	1.13	50 ± 3 54 ± 4	–	65 ± 2	^{1}H BSATD-LIS* ^{13}C BSATD-LIS*	0.11 (^{1}H) 0.02 (^{13}C)	[129, 133]
$[Nd(H_2O)_n(DOTA)]^-$	1.11	–	–	–	^{13}C	0.1$^{\&}$	[70]
$[Eu(H_2O)_n(DOTA)]^-$	1.09	64 ± 1	61 ± 3	–	^{1}H 1D EXSY	-	[134]
$[Eu(DOTAM)]^-$	1.09	54.6	–	–	^{1}H BSA^b	-	[71]
$[Ho(H_2O)_n(DOTA]^-$	1.04	65 ± 3	–	–	^{1}H BSATD-LIS*	1.46 (^{1}H)	[69]
$[Tm(DOTP)]^{2-}$	1.02	–	–	–	^{1}H NMR	1.17$^{\&}$	[87]
$[Yb(H_2O)_n(DOTA)]^-$	1.01	65.7 ± 1.3	61.6 ± 1.1	65.9 ± 1.0	^{1}H 2D EXSY	0.22$^{\&}$(^{1}H)	[119]
$[Lu(H_2O)_n(DOTA)]^-$	1.00	62.7 ± 2.0	58.7 ± 2.1	65.9 ± 1.2	^{1}H and ^{13}C BSA$^{\#}$	0.0$^{\&}$(^{1}H)	[60]

$^{\#}$BSA means band shape analysis technique within the framework of the dynamic NMR

*BSATD-LIS means band shape analysis taking into account temperature dependence of LIS within the framework of the dynamic NMR

$^{\&}$Our calculations

The value of the enthalpy ΔH^o corresponding to the thermodynamic equilibrium between the SAP and TSAP isomers decreases with the transition from Ho to Lu in the lanthanide series (Table 5).

The decrease in ΔH^o in the series of lanthanide complexes $[Ln(H_2O)_n(DOTA)]^-$ could be owing to the effect of "lanthanide compression", since the radius decreased of the cationic from La to Lu in lanthanide complexes.

One can see some features by comparing the intramolecular dynamics taking place in complexes of lanthanides with folder ligands and with crown ethers. In particular, one can see that the activation free energy of the inversion of crown ether in beta-diketonate lanthanide complexes is almost independent of the radius of the metal cation. This could be owing to the fact that the inversion process is limited by its own internal processes of the crown ether molecule. In this case, the found activation energy of the dynamics coincides with the activation energy of the conformational inversion of the free ligand itself (about 65 kJ mol^{-1}). The proposed mechanisms of dynamics are discussed in detail in [8]. Briefly characterize the mechanism, we can note the following. Before the inversion, most coordination bonds of Ln–O (18-crown-6) break. Then, the molecule is inverted, followed by the restoration of all Ln–O bonds. On the contrary, a monotonic decrease in the activation energy of conformational inversion (with an increase in the atomic number of the Ln cation) is observed in the complexes $[Ln(NO_3)_3(18\text{-crown-6})]$. This decrease in the activation energy of conformational inversion could be owing to the effect of lanthanide compression. It can be assumed that the Ln cation exerts a catalytic decrease in the energy barrier of conformational inversion in the $[Ln(NO_3)_3(18\text{-crown-6})]$ complexes with a decrease in the ionic radius of the metal.

As one can see from Table 6, the activation energy of conformational dynamics in lanthanide complexes with various derivatives of DOTA is about 60 kJ mol^{-1}. The results presented in Table 6 have been obtained by various methods

Table 7 Chemical shifts (ppm) and assignment of signals of the complexes $[Ln(H_2O)_n(DOTA)]^-$ (LnL) in ^1H NMR spectra (Ln = Eu, Ho, Yb) [139]

Signal assignment	Chemical shifts (ppm)		
	EuL	HoL	YbL
SAP isomer			
ax1	36.5	− 242.6	133
ax2	− 10.7	86.9	− 47
e1	− 1.9	− 55.4	24
e2	− 8.0	− 55.4	20
ac1	− 17,3	53.6	− 38
ac2	− 19.5	161.0	− 82
TSAP isomer			
ax1*	13.6	− 124.0	80
ax2*	− 2.4	53.5	− 32
e1*	− 8.7	− 35.6	15
e2*	− 11.2	− 34.7	10
ac1*	− 4.2	39.3	− 25
ac2*	− 6.1	104.5	− 54

Table 6 Kinetic data for ring inversion and other types of dynamics in macrocyclic lanthanide complexes as studied by dynamic NMR techniques and CD*

Complex	$\Delta H^{\ddagger}$ or $\Delta G^{\ddagger}(T)$, kJ mol^{-1}	Type of dynamics	$k_{ex}(T)$, s^{-1}	Solvent	Nucleus, techniques	Refs
$[Pr(NO_3)_3$(diaza-18-crown-6)]	$\Delta H^{\ddagger} = 22$	IE	–	CD_2Cl_2	^1H, BSATTD-LIS	[134, 135]
$[Pr(NO_3)_3(18\text{-crown-6})]$	$\Delta H^{\ddagger} = 26$	IE, PR	–	CD_2Cl_2	^1H, BSATTD-LIS	[136, 137]
$[Ce(NO_3)_3(18\text{-crown-6})]$	$\Delta G^{\ddagger}$ (320 K) = 28 $\Delta G^{\ddagger}$ (320 K) = 58	IE, PR RI	–	$CD_2Cl_2/CDCl_3$	^1H, BSATTD-LIS	[130, 134]
$[Pr(NO_3)_3(18\text{-crown-6})]$	$\Delta G^{\ddagger}$ (320 K) = 39 $\Delta G^{\ddagger}$ (320 K) = 49	IE, PR RI	–	CD_2Cl_2	^1H, BSATTD-LIS	[137]
$[Nd(NO_3)_3(18\text{-crown-6})]$	$\Delta G^{\ddagger}$ (320 K) = 33 $\Delta G^{\ddagger}$ (320 K) = 45	IE, PR RI	–	$CD_2Cl_2/CDCl_3$	^1H, BSATTD-LIS	[130]
$[Pr(fod)_2(18\text{-crown-6})]^+$	$\Delta G^{\ddagger}$ (363 K) = 74	RI	–	$CDCl_3$	^1H, BSATTD-LIS	[138]
$[La(DOTTEA)]^{3+}$	$\Delta G^{\ddagger}$(298 K) = 58.8	RI	300 (298 K)	H_2O/CD_3CN	^{13}C, BSA	[57]
$[La(DOTEAM)]^{3-}$	$\Delta G^{\ddagger}$(298 K) = 58.9	RI	–	H_2O/CD_3CN	^{13}C, BSA	[129]
[La(DO2AMeIm)]	$\Delta G^{\ddagger}$(298 K) = 62.6	RI	107 (298 K)	H_2O/CD_3CN	^{13}C, BSA	[130]
$[(R)\text{-}Eu(gDOTA)]^{5-}$		ARF(M to m) ARF(m to M)	45 (293 K) 11 (293 K)	H_2O/CD_3CN	^1H, MT	[110]
$[Eu(DTMA)]^{3+}$	$\Delta G^{\ddagger}$(298 K) = 62.2	RI(M to m) RI(m to M)	80 (298 K) 430 (298 K)	H_2O/CD_3CN	^1H, MT, 2D-EXSY	[42]
$[Eu(DOTMAM)]^{3+}$	$\Delta G^{\ddagger}$(298 K) = 62.5	ARF(M to M) ARF(m to M)	230 (298 K) 70 (298 K)	H_2O/CD_3CN	^1H, MT	[42]

and are completely mutually consistent. It should be noted that the kinetics (on a NMR time scale) of reversible chemical reactions in paramagnetic lanthanide complexes is quite possible to quantify using the band-shape analysis technique taking into account temperature dependence of LIS [128–131], a homonuclear double resonance NMR techniques (SST, MT and 2D EXSY [42, 44].

Equilibrium constants K_T=[TSAP]/[SAP], where [TSAP] and [SAP] is concentrations of conformers TSAP and SAP, respectively.

Here BSA is the band-shape analysis within the framework of dynamic NMR. BSATTD-LIS means the use of the band-shape analysis technique taking into account temperature dependence of LIS. SST is spin saturation transfer technique. CD* is the circular dichroism (the differential absorption of left and right circularly polarized light). PRR is the phenyl ring rotation. IE is the interconversion of enantiomers. PR is pseudorotation. RI is the ring inversion. ARF is arm rotation frozen. RDR is the rotation of the decker rings. MT is the selective magnetization transfer method. EXSY is the exchange spectroscopy. *M* and *m* refer to square-antiprismatic (SAP) and twisted square-antiprismatic (TSAP) isomeric structures.

Table 8 Lanthanide-induced splittings ($\Delta\delta$, ppm) of the ^{1}H NMR signals of diastereotopic protons of various groups of macrocyclic ligands and the structural type of molecules in Ln complex compounds at ambient temperature

Compound	Ln	Solvent	Inclusion type structure	Kinetic stability	Groups	$\Delta\delta$, ppm	Refs
$[Ln(ClO_4)_3$(12- crown-4)]	Tm	CD_3CN	+	+	CH_2	215	[140]
$[Ln(NO_3)_3$(DCH-18-crown-6)]	Pr	$CD_3CN/CDCl_3$	+	+	CH_2	5	[141]
$[Ln(NO_3)_2$(DA-18-crown-6)]$^+$ Eu	Eu	$CDCl_3$	+	+	CH_2	57	[138]
$[Ln(L)_2$(18-crown-6)]$^+$	Ce	CD_3CN; CD_2Cl_2	+	+	CH_2	0.6	[129]
	Pr	CD_3CN	+	+	CH_2	2	[129]
	Nd	CD_3CN	+	+	CH_2	0.6	[129]
	Eu	CD_3CN	+	+	CH_2	0.8	[129]
$[Ln(NO_3)_3$(18-crown-6)]	Pr	CD_3CN; CD_2Cl_2	+	+	CH_2	10	[142]
$[Ln(L)_2$(DB-18-crown-6)]$^+$	Pr	CDC_{l3}	+	+	CH_2	6.7	[129]
[Ln (MOFPP)$_2$]	Ce	DMSO-d6	+	+	C_6H_2-$(OMe)_2$	3.12	[143]
(RRRR)-[Ln(S)]	Eu	CD_3CN/H_2O	+	+	CH_2	46.8	[110]
	Yb	CD_3CN/H_2O	+	+	CH_2	133.5	[110]
$[Ln(H_2O)_n$(DOTA)]$^-$	Ho	D_2O	+	+	CH_2	187	[69]
	Yb	D_2O	+	+	CH_2	109	[119]

Here *L* is ptfa anion, *L'* is hfa anion, MOFPP is 5,15-bis(3,5-dimethoxyphenyl)-10,20-bis(pentafluorophenyl) porphine, S is 1,4,7,10-tetrakis(carboxyethyl)-1,4,7,10-tetraazacyclododecane

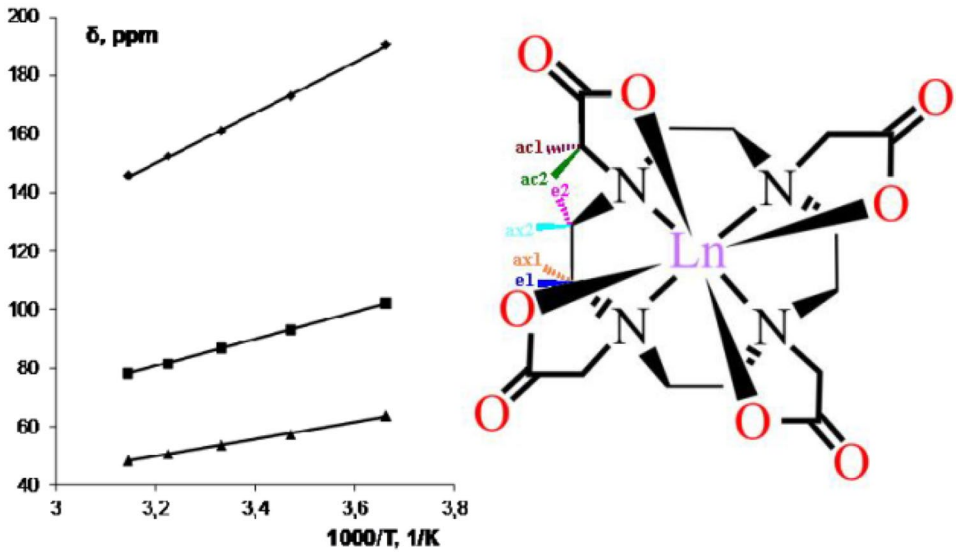

Fig. 15 Temperature dependence of paramagnetic LIS of the complex $[Ho(H_2O)_n(DOTA)]^-$ in 800 MHz ^{1}H NMR spectra. ac2 (◆), ax2 (*), ac1 (▲) are signals of SAP conformer, solvent is D_2O [69]

To verify the correctness of $[Ln(H_2O)_n(DOTA)]$ (Ln = Eu, Ho, Yb) signal assignments in the NMR spectra the analysis of paramagnetic LIS has been made by using corresponding NMR spectral data according to [139] (Table 7).

It could be noted that in the $[Ln(H_2O)_n(DOTA)]^-$ complexes there is a large-scale splitting between diastereotopic protons ("ax1"- "e1" and "ax2"- "e2" pairs). It has been previously noted [8] that such a splitting indicates that the complex is inclusive and kinetically stable. Table 7 lists several Ln complexes with MCPE, porphyrins and DOTA-like molecules whose spatial structure in solution has been studied in detail. The data in the Table 7 show that the detection of lanthanide-induced splitting of diastereotopic protons of different groups of macrocyclic ligand molecules is sufficient for the detection of kinetically stable complexes of these macrocycles with lanthanide cations having the structure of inclusive type both for lanthanide complexes with crown ether in organic solutions, and for DOTA complexes in aqueous media. It should be noted that Table 8 shows only a few examples when the lanthanide-induced splitting of diastereotopic protons is zero. However, such examples could be given significantly more than shown in Table 8.

Temperature dependences of paramagnetic LIS for signals of hydrogen atoms of different CH_2 groups in complex of $[Ho(H_2O)_n(DOTA)]^-$ are shown in Fig. 15 [69].

As shown in Fig. 15, the dependence of LIS (δ^{obs}-δ^{dia}) with respect to $1/T$ is linear (Eq. 29) [8]:

$$\delta^{\mathrm{obs}} - \delta^{\mathrm{dia}} = \mathrm{a} + \mathrm{b}/T, \tag{28}$$

Moreover, the linear dependence of LIS versus reverse temperature (most of the experiments in the 200 K to 350 K temperature range occured) is observed for the majority of Ln complexes, such as the complexes $[Ln(H_2O)_n(EDTA)]^-$ (Ln = Pr, Er, Ho, Tm and Yb) [94–99]. The signal of the H atom «ac2» (161 ppm at 300 K) of the $[Ho(H_2O)_n(DOTA)]^-$ complex has a maximum LIS sensitivity $d(\Delta\delta_{ex})/dT = 1.46$ ppm/K. The temperature sensitivity $d(\Delta\delta_{ex})/dT$ for the signal «ac2» is much higher than the temperature sensitivity of the chemical shift of pure water (about 0.01 ppm/K). It should also be noted that the value of $d(\Delta\delta_{ex})/dT = 1.46$ is greater than many other lanthanide complexes of PAPC ligands, including the complex of $[Tm(DOTP)]^{2-}$ [85].

Lanthanide complexes with DTPA-like ligands

Aminopolycarboxylates have been extensively studied [100, 138, 139, 140, 141, 142, 143144, 147, 148, 149, 150], and their high affinity for metal coordination is utilized in a wide spectrum of industrial products such as agrochemicals, cleaners, detergents, bleaching agents, and magnetic resonance imaging contrast agents [101, 145]. Perhaps the most well-known reagent in this family, DTPA has been first used by Orr in an eluent mixture to efficiently separate trivalent americium from promethium using an ion-exchange method [152]. Later Weaver and Kappelmann used DTPA as an aqueous holdback reagent in a liquid – liquid formulation known as the TALSPEAK (Trivalent Actinide – Lanthanide Separation by Phosphorus reagent Extraction from Aqueous Komplexes) process. [153, 154]. Recently, a lot

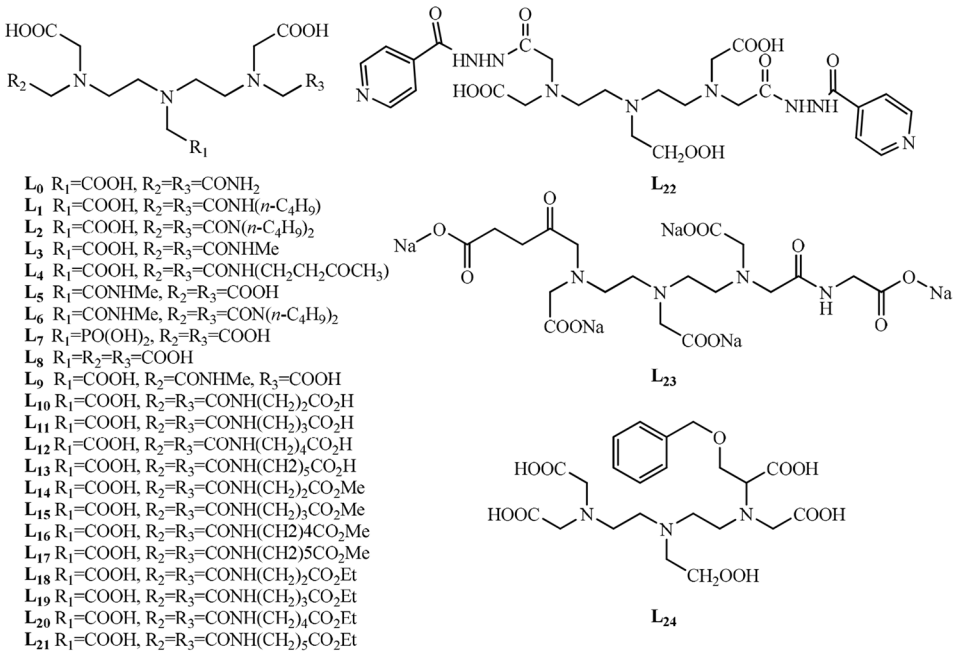

Fig. 16 The structure of DTPA and novel DTPA derivatives

of novel DTPA derivatives have been synthesized [155, 156, 157, 158, 159, 160, 161] such as DTPA-BMA (DTPA-bis(methyl)-amide) and other derivatives with various alkyl or aryl groups [162–170] some novel macrocyclic DTPA bis(amide) derivatives [171–173], and derivatives with the replacement of the two terminal carboxylates of $DTPA^{5-}$ with the non-ionic amide groups [174, 175]. The structures of DTPA and DTPA derivatives have been shown in Fig. 16.

In recent years we can mention that the lanthanide complexes (Ln) with DTPA and with DTPA-amide derivatives have attracted considerable interest. This is a consequent of the successful application of $[Gd(DTPA)]^{2-}$ as a contrast agent in magnetic resonance imaging (MRI) for the enhancement of proton relaxation rates [15, 170–179]. The potential of $[Ln(DTPA)]^{2-}$ complexes as contrast agent for magnetic resonance imaging (MRI CA) must be investigate taking into account some relevant physicochemical properties such as (i) the protonation constants; (ii) thermodynamic and conditional stability constants; (iii) the selectivity for the Ln(III) ion over the endogenous metal ions such as Zn(II), Ca(II), and Cu(II); (iv) the relaxivities in aqueous solutions, which express the efficacy of a Ln^{3+} complex to increase the relaxation rate of water protons.

Various MRI agents currently available for clinical uses could be divided into the two types such as anionic $[Gd(DTPA)(H_2O)]^{2-}$ and neutral [Gd(DTPA-bisamide)(H_2O)] complexes. Among the two complexes, although the first commercially available contrast agent represents the dimeglumine salt of $[Gd(DTPA)(H_2O)]^{2-}$ [180] the latter is preferred because of a relatively low osmotic pressure in body fluids after intravenous administration [175].

Cacheriset et al. assumed that, although the dissociation of $[Gd\mathbf{L_3}(H_2O)]$ ($\mathbf{L_3}$ ligand shown in Fig. 16) is fast and a complexation equilibrium exists in body fluids, the high selectivity of the $DTPA\text{-}BMA^{3-}$ provides an in vivo safety of the injected contrast agent [169]. However, more recently it has been found that the kinetic stability of $[Gd\mathbf{L_3}H_2O)]$ and related Gd-DTPA-bis(amide) complexes is high and comparable to that of $[Gd(DTPA)(H_2O)]^{2-}$[182, 183]

This finding also implies that stability constants and selectivity level play a minor role in determining nontoxicity for a contrast agent; the crucial factor undoubtedly consists in a high kinetic stability [182–184].

High kinetic stability represents an important requirement for Ln complexes used as contrast enhancement agents in magnetic resonance imaging. The kinetic stabilities of the Ln complexes formed with DTPA derivatives are characterized by the rates of exchange reactions with Ln and with endogenous Cu and Zn. The exchange reactions occur via the proton-assisted dissociation of the complexes and via a direct attack of the exchanging metal ions on the complex.

The kinetic stability of the $[Gd(L^3)]^+$ complexes can be characterized by the rate of exchange (transmetallation) reactions as it follows [184–188]:

$$GdL + M^{n+} = ML^{(n-3)+} + Gd^{3+} \tag{29}$$

where L is DTPA or such derivatives as L_0-L_6; M^{n+} is the exchanging metal ion, for example Eu^{3+}, Cu^{2+} or Zn^{2+}.

In the presence of a large excess of M^{n+} the exchange reaction rate can be expressed by Eq. (30)

$$-\frac{d[GdL]_t}{dt} = k_{obs}[GdL]_t \tag{30}$$

where *kobs* is a pseudo-first-order rate constant and $[GdL]_t$ is the total concentration of Gd^{3+} complex.

E. Tóth and E. Brücher explored the kinetic inertness of $[Gd(L^3)]^+$ by studying exchange reactions with Eu^{3+}, Zn^{2+} and Cu^{2+}, characterized the exchange reaction rates by varying the concentration of the H^+ or M^{n+} ions for obtaining the rate law, and determined the rate and mechanism of water exchange on the Gd^{3+} complex, combining variable temperature and pressure in ^{17}ONMR and EPR studies [180, 181]. The rate constants k_1, k_3 and k_4, and the stability constant K_{GdLM} obtained in the fit are shown in Table 9.

Table 9 Rate constants characterizing the exchange reactions between the Gd^{3+} complexes of the DTPA-amide derivative ligands and Eu^{3+},Cu^{2+} or Zn^{2+} (25°C, 1.0 M KCl)

Exch. ion	Rate constant/M^{-1} s^{-1}	L_8 [a]	L_5 [b]	L_2 [c]	L_6 [d]
Eu^{3+}	k_1	0.58	1.6	0.23	0.38 ± 0.02
	k_3	4.9×10^{-4}	3.4×10^{-3}		$(1.4 \pm 0.2) \times 10^{-4}$
	k_4				5.0 ± 0.7
Cu^{2+}	k_1	0.58	1.6	0.28	0.40 ± 0.09
	k_3	0.93	0.62	7.3×10^{-2}	$(6.3 \pm 0.1) \times 10^{-2}$
Zn^{2+}	k_1	0.58	0.6	0.21	0.5 ± 0.15
	k_3	5.6×10^{-2}	8.1×10^{-2}	1.57×10^{-3}	$(8.7 \pm 0.3) \times 10^{-3}$
	k_4			29	110 ± 10

[a]Ref. [189, 190]..b: Ref. [183]; c: Ref. [187]; d: Ref [186]. where $k_1 = k_{GdHL}K_{GdHL}$, $k_3 = k_{GdLM}K_{GdLM}$ and $k_4 = k_{HGdLM}K_{GdLM}$. K_{GdHL} the protonation constant; K_{GdLM}: stability constant ($K_{GdLM} = [GdLM]/[GdL][M]$)

All the rate constants for the proton assisted dissociation (k_1) are rather similar for $[Gd(\mathbf{L_0})]^{2-}$, $[Gd(\mathbf{L_2})]$ and $[Gd(\mathbf{L_3})]^{+}$, but for $[Gd(\mathbf{L_1})]^{-}$ the k_1 value is about three times higher. This means that the carboxylate-to-amide substitution on the terminal and central nitrogens at $(\mathbf{L_0})^{5-}$ exerts no significant effect on the rate of the proton assisted dissociation of the Gd^{3+} complexes. The positively charged complex $[Gd(\mathbf{L_3})(H_2O)]^{+}$ has a lower thermodynamic stability constant than the parent $[Gd(DTPA)(H_2O)]^{2-}$ or some Gd^{3+} complexes with DTPA-bis(amide). In contrast to the thermodynamic stability, the kinetic inertness of $[Gd(\mathbf{L_3})]^{+}$, characterised by the rates of metal exchange reactions with Eu^{3+}, Cu^{2+} and Zn^{2+} ions, is higher.

The exchange reactions occur via proton- and metal ion assisted dissociation of $[Gd(\mathbf{L_3})]^{+}$.

These reactions are slower for $[Gd(L_3)]^{+}$ than for $[Gd(DTPA)]^{2-}$, since the amide groups cannot be protonated and interact only weakly with the attacking metal ions. The rate of water exchange on $[Gd(L_2)(H_2O)]$ and $[Gd\text{-}(\mathbf{L_3})(H_2O)]^{+}$ is reduced in comparison to $[Gd(DTPA)(H_2O)]^{2-}$. This is explained by the lower negative charge and decreased steric crowding at the water binding site in amides as compared to carboxylate analogues. The activation volumes evidence a dissociative interchange and a limiting dissociative mechanism for $[Gd(\mathbf{L_2})(H_2O)]$ and $[Gd(\mathbf{L_3})(H_2O)]^{+}$, respectively.

High solubility in water alongside with non-toxicity is an essential criterion for the practical application as MRI CA. In additioN,Nowadays there is a variety of DTPA-bis(amide) ligands known, many of which carry aromatic or large aliphatic substituents, thus resulting in poor solubility in water upon complexation with Gd [158, 160, 165, 167, 189–192].

Relaxivities express the efficacy of a Ln^{3+} complex to increase the relaxation rate of water protons. Usually, the relaxivity (r_1) of complexes and $Gd(DTPA)^{2-}$ used as the reference have been determined.

As example we can mention that the relaxivity of $M\mathbf{L_{22}}$, (M: La, Sm, Eu, Gd, Tb) and $Gd(DTPA)^{2-}$ have been 0.14, 1.66, 3.14, 6.08, 2.79 and 4.34 $l{\cdot}mmol^{-1}{\cdot}s^{-1}$, respectively, which have been reported by Z. Y. Yang [193]. The spin–lattice relaxivity of $Gd\mathbf{L_{22}}$ has been larger than that of $Gd(DTPA)^{2-}$. The relaxivity of GdL had also been investigated in human serum albumin (HSA) solution, and the

Table 10 Relaxivity of the Complexes [192, 193]

Compound	[M]/ mol· l^{-1}	t_0/s	T_1/s	$(1/T_1)_p/s^{-1}$	r_1/mmol·l·s^{-1}
H_2O+D_2O		5.40	0.128		
$La\mathbf{L_{22}}{\cdot}2(H_2O)$	0.093	4.90	0.141	0.013	0.14
$Sm\mathbf{L_{22}}{\cdot}2(H_2O)$	0.097	2.40	0.289	0.161	1.66
$Eu\mathbf{L_{22}}{\cdot}4(H_2O)$	0.097	1.60	0.433	0.305	3.14
$Gd\mathbf{L_{22}}{\cdot}5(H_2O)$	0.099	0.95	0.730	0.602	6.08
$Tb\mathbf{L_{22}}{\cdot}2(H_2O)$	0.092	1.80	0.385	0.257	2.79
Gd-DTPA	0.148	0.90	0.770	0.642	4.34

Table 11 Relaxivity data of $[Gd(\mathbf{L_x})(H_2O)]{\cdot}xH_2O$ in aqueous and aqueous HP-b-CD solutions [194, 195]

Complexes	r_1 (mM^{-1} s^{-1})	r_2 (mM^{-1} s^{-1})	r_1 [a] (mM^{-1} s^{-1})	r_2 [a] (mM^{-1} s^{-1})
$[Gd(\mathbf{L_{10}})(H_2O)]{\cdot}xH_2O$	1.58	1.50	9.4	9.7
$[Gd(\mathbf{L_{11}})(H_2O)]{\cdot}xH_2O$	1.43	1.23	10.4	11.0
$[Gd(\mathbf{L_{12}})(H_2O)]{\cdot}xH_2O$	1.31	1.00	8.6	8.7
$[Gd(\mathbf{L_{13}})(H_2O)]{\cdot}xH_2O$	1.44	1.23	11.6	12.1
$[Gd(\mathbf{L_{14}})(H_2O)]{\cdot}xH_2O$	1.59	1.71	8.7	8.8
$[Gd(\mathbf{L_{15}})(H_2O)]{\cdot}xH_2O$	1.54	1.35	8.8	8.9
$[Gd(\mathbf{L_{16}})(H_2O)]{\cdot}xH_2O$	1.47	1.31	9.1	9.2
$[Gd(\mathbf{L_{17}})(H_2O)]{\cdot}xH_2O$	1.65	1.52	12.6	13.0
$[Gd(\mathbf{L_{18}})(H_2O)]{\cdot}xH_2O$	1.95	1.94	10.1	10.4
$[Gd(\mathbf{L_{19}})(H_2O)]{\cdot}xH_2O$	1.71	1.63	12.2	12.5
$[Gd(\mathbf{L_{20}})(H_2O)]{\cdot}xH_2O$	1.68	1.65	10.4	10.5
$[Gd(\mathbf{L_{21}})(H_2O)]{\cdot}xH_2O$	1.54	1.40	10.5	10
Gd(DTPABMA)	4.58	4.76	-	-
$[Gd(DTPA)]^{2-}$ [b]	3.40	3.80	-	-

[a]In [HP-b-CD] = 50 mM; b: $[Gd(DTPA)]^{2-}$, r_1 and r_2 measured at $B_0 = 1.0$ T; $[Gd(\mathbf{L_x})(H_2O)]{\cdot}xH_2O$: $\mathbf{L_x}$: $\mathbf{L_{10}} - \mathbf{L_{21}}$

relaxivity of GdL has been enhanced from 6.08 l·mmol^{-1}·s^{-1} in water solution to 9.09 l mmol^{-1}·s^{-1} in HSA solution.

The relaxation rate enhancement value of the complex for water protons can be calculated according to Eqs. (32, 33) [187].

$$\left(1/T_1\right)_p = \left(1/T_1\right)_o - \left(1/T_1\right)_d, \tag{31}$$

$$r_1 = \left(1/T_1\right)_p/[M], \tag{32}$$

where $(1/T_1)_o$ is the observed solvent relaxation rate in the presence of a paramagnetic species; $(1/T_1)_d$ is the solvent relaxation rate in the absence of a paramagnetic species; $(1/T_1)_p$ represents the additional paramagnetic contribution; [M] is the concentration of paramagnetic metal ion.

The high relaxivity is favourable of tissue imaging. The relaxivity (r_1) of complexes and $[Gd(DTPA)]^{2-}$ used as the reference are given in Table 10. The results showed that the spin–lattice relaxivity of Gd**L**$_{22}$ has been larger than that of $[Gd(DTPA)]^{2-}$.

Other example of the selectivity of DTPA-bis(amide) ligands for the Gd(III) ion over the endogenous metal ions such as Zn(II), Ca(II), and Cu(II), and relaxivities (r_1 and r_2) of Gd(III)-DTPA-bis(amide) complexes both in aqueous and hydroxypropyl-b-cyclodextrin (HP-b-CD) solutions reported by T. J. Kim [194]. HP-b-CD is biocompatible and has been used in the preparation of aqueous solution of water-insoluble drugs [195]. The relaxivities (r_1 and r_2) of $[Gd(\mathbf{L}_x)(H_2O)]\cdot xH_2O$ ($\mathbf{L_x}$**: L$_{10}$-L$_{21}$**) in aqueous and aqueous HP-b-CD solutions are collected in Table 11. Relaxivities (r_1 and r_2) have been calculated as an inverse of relaxation time per mM.

In aqueous solutions, the complexes formed by Gd with ligands (**L$_{10}$-L$_{21}$**) show significantly lower relaxivities than analogous Gd(III) complexes of DTPA-BMA and DTPA.

In addition, the relaxivities (r_1 and r_2) of aqueous solutions of $[Gd(\mathbf{L}_x)(H_2O)]\cdot xH_2O$ ($\mathbf{L_x}$**: L$_{10}$-L$_{21}$**), drop significantly as compared with $[Gd(DTPA\text{-}BMA)(H_2O)]$ although they increase dramatically (6–tenfold) in aqueous hydroxypropyl-b-cyclodextrin (HP-b-CD) solution.

It is known that a significant increase in relaxivity is established when ''host–guest'' inclusion complexes are formed between the hydrophobic b-cyclodextrin cavity

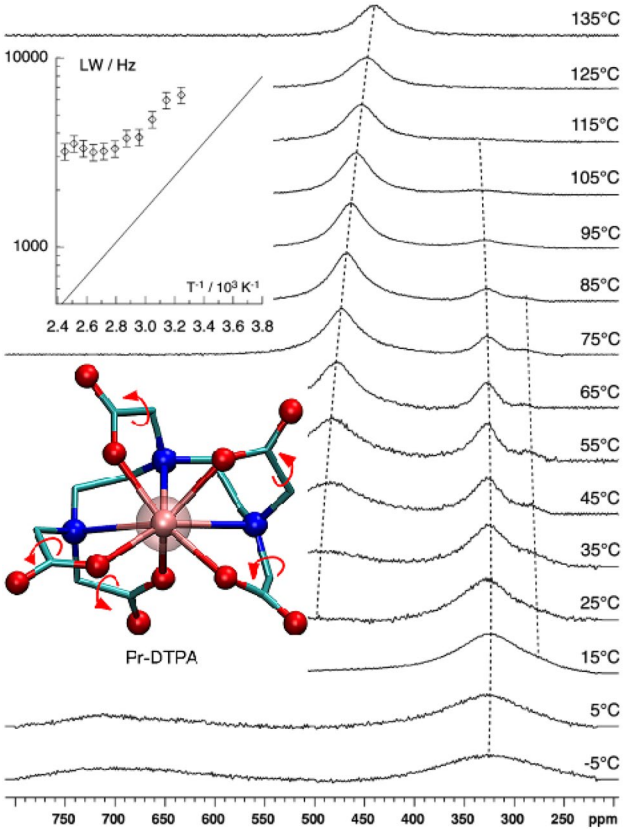

Fig. 18 Variable temperature ^{17}O NMR spectra registered at 14.1 T for the Pr-DTPA complex in aqueous solution [205]. No apodization of the free induction decay has been used. The dotted lines are guides for the eye emphasizing chemical shift variations. The variation of the full line width at half-height versus the inverse temperature (35 − 135 °C) is shown in the inset for the signal at 500 − 450 p.p.m. as a semilogarithmic plot; the confidence intervals correspond to ± 10% (twice the estimated relative standard error). For comparison purpose, the data for Sm-DTPA line width are shown as a plain line

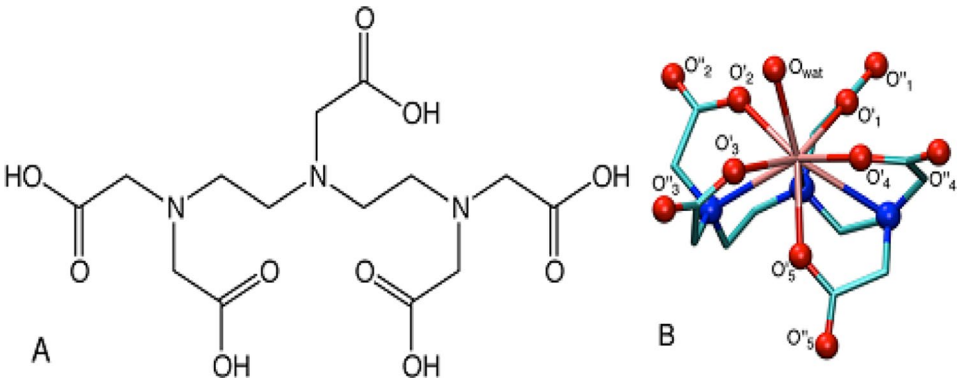

Fig. 17 Structure of the DTPA ligand (**A**), ball-and-stick representation of a metal-DTPA complex (**B**). In part B, the hydrogen atoms are omitted for clarity, the nitrogen atoms are shown in blue, and the oxygen atoms in red; the oxygen atoms coordinated to the metal ion are labeled as O′and the noncoordinated carbonylic oxygen atoms as O″

of hydroxypropyl-b-cyclodextrin (HP-b-CD) and Gd(III) complexes [186, 196].

In this regard, the aliphatic amide side-arms in [Gd($\mathbf{L_x}$)(H_2O)]·xH_2O ($\mathbf{L_x}$**:** $\mathbf{L_{10}}$-$\mathbf{L_{21}}$) are expected to interact with the hydrophobic cavities of the b-CD moieties of HP-b-CD thus leading to the formation of ''host–guest'' complexes. Indeed, a dramatic increase in r_1 and r_2 values are to be noted. These observations demonstrate that the inclusion has truly taken place between [Gd($\mathbf{L_x}$)(H_2O)]·x(H_2O) ($\mathbf{L_x}$**:** $\mathbf{L_{10}}$-$\mathbf{L_{21}}$) and HPb-CD.

The structure and conformatoional dynamics of Ln-DTPA complexes have been the subject of several studies by X-ray diffraction and/or nuclear magnetic resonance (NMR) [94, 197–204].

X-ray structural studies on the Ln^{3+} complexes of some DTPA bis(amide) derivatives have revealed that the ligands are coordinated to the Ln^{3+} via three acetate oxygens, three nitrogen atoms and the two carbonyl oxygens of the amide groups. The ninth coordination site is occupied by an H_2O molecule [155, 158–160]. The multiplicity of the ^{1}H NMR spectra observed first by Geraldes et al. [163] points to the existence of several conformational isomers [155, 173, 175]. The results of ^{1}H and ^{13}C NMR studies indicate that the structures of the Ln^{3+} DTPA bis(amide) complexes in aqueous solution are similar to their solid-state structures. The generic structure of $[Ln(DTPA)]^{2-}$ complexes is depicted in Fig. 17.

By the example, we could mention the DTPA chelates of various diamagnetic and paramagnetic lanthanide(III) metal ions, as well as a chemically similar DTPA chelate of Y^{3+}, in an aqueous solution. The internal dynamics of the Y-DTPA chelate and various Ln-DTPA chelates have been investigated in aqueous solution by variable temperature ^{17}O NMR by L. Fusaro [205] (As shown in Fig. 18). As a consequence of poor chemical shift dispersion and fast quadrupole relaxatioN,No kinetic data could be obtained for the chelates of the diamagnetic La^{3+}, Lu^{3+}, and Y^{3+} metal ions nor for the chelate of the weakly paramagnetic Sm^{3+} ion.

However, the apparent activation energy characterizing the overall rotational dynamics, as determined from the temperature dependence of the line width, have been found to be in excellent agreement with the literature data. The ^{17}O NMR spectra show several signals for the Pr-DTPA and Eu-DTPA complexes and reveal that these compounds are fluxional as a consequence of both the racemization process and the interchange of the coordinated and noncoordinated oxygen atoms of the carboxylate group. The fluxional behavior of the carboxylate groups is, however, not expected to significantly affect the residence time of the water molecule coordinated to the metal ion. The spectra registered for the Eu-DTPA complex show chemical exchange owing to the well-known racemization process and, at high temperature, feature signal broadening that reveals a fluxional process involving the interchange of the coordinated and noncoordinated oxygen atoms of the carboxylate groups. The free energy barriers of both the Pr-DTPA and Eu-DTPA complexes are remarkably lower than the calculated values recently reported by Mayer et al. for a series of Ln-DOTA complexes [115], and are somewhat greater than the activation free energy characterizing the racemization of these DTPA chelates, which, on the order of 60 kJ mol^{-1}. Furthermore, the smallest activation free energy measured for the Pr-DTPA complex, about 45 kJ mol^{-1}, is significantly lower than the activation free energy characterizing the racemization process. However, these values are significantly higher than the activation free energy characterizing the exchange of the water molecule coordinated to the metal ion, which corresponds to a value of 35 kJ mol^{-1}, suggesting that the two processes are independent.

Previously, intramolecular conformation dynamics of $[Ln(H_2O)_n(DTPA)]^{2-}$ complexes in case of Pr^{3+}, Eu^{3+} and

Table 12 Activation free energies ($\Delta G^{\ddagger}_{298}$, kJ mol^{-1}), temperature derivative of experimental lanthanide-induced shifts ($\partial\delta(T)/\partial T$, ppm/K) and methods used for the investigation of intramolecular dynamics in $[Ln^{3+}(H_2O)_n(DTPA)]^{2-}$ complexes

Lanthanide Ion	Radius/Å	Activation Energy/ (kJ mol^{-1})	Method	$\partial\delta(T)/\partial T$, ppm/K	solvent	Ref
Pr^{3+}	1.13	57 ± 4	^{1}H EXSY-CT [a]	–	D_2O;D_2O/CD_3OD	[14]
		60	^{17}O BSA [b]	1.1 (^{17}O)	D_2O	[205]
		53 ± 5	^{1}H BSATTD-LIS	0.17	D_2O	[207]
Eu^{3+}	1.09	55 ± 5	^{1}H EXSY-CT	–	D_2O	[14]
		55	^{17}O BSA		D_2O	[205]
		64 ± 5	^{1}H BSATTD-LIS[c]	0.11	D_2O	[207]
Ho^{3+}	1.04	66 ± 5	^{1}H BSATTD-LIS[c]	0.64	D_2O	[207]
Yb^{3+}	1.01	49 ± 10	^{1}H EXSY-CT	–	D_2O	[14]
		45 ± 5	^{1}H BSATTD-LIS[c]	0.43	D_2O	[207]

[a]EXSY-CT means a combined approach based on 2D EXSY and NMR "determining coalescence temperatures"; b: BSA means band-shape analysis; c: BSATTD-LIS means band-shape analysis technique taking into account the temperature dependence of LIS.

Yb^{3+} have been studied by a combined approach based on ^{1}H 2D EXSY and NMR by R. Lauffer [14].

The conformational dynamics of $[Ln(H_2O)(DTPA)]^{2-}$ complexes ($Ln = Pr^{3+}$, and Eu^{3+}) has been also investigated by L. Fusaro as mentioned above [205]. Although, the two types of conformational dynamic processes have been identified by ^{17}O NMR, the first one is conditioned by rotation of the carboxylate fragment, and the second one is conditioned by the enantiomerization. However, there are some differences between the values of the free energy of activation of conformational racemization, obtained by these two different methods. S.P. Babailov have previously proposed a method for studying the conformational dynamics of Ln complexes, based on the shape of the NMR signal analysis, taking into account temperature changes in paramagnetic LIS (BSATTD-LIS) [200, 201]. Meanwhile, comparison of results obtained by three methods for complexes Pr^{3+} (I), Yb^{3+} (II) and Ho^{3+} (III) with DTPA by using ^{1}H NMR (withing the framework of BSATTD-LIS) and studies on the intramolecular racemization and more detailed study the substantial temperature dependence of LISs has been carried out [207] (as shown in Table 12).

It should be noted that the approach based on the line shape analysis taking into account the temperature variation of LIS for the first time has been applied to the investigation of the complexes of holmium. The determination of the rate constants of the processes and the free energy of activation is similar in the case of the three methods. As it can be seen from Table 11 for complexes of Pr to Ho the free activation energy of intramolecular dynamics slightly increases with decreasing lanthanide cation radius. This monotonic increase in the activation free energy of conformational racemization in a series of Ln is consistent with the results of studies in other complexes {interconversion of conformers} in the $[Ln(H_2O)(DOTA)]^{-}$ complexes [65] intermolecular dynamics in $[Ln(H_2O)_n(DTPA)]^{2-}$ for the yttrium subgroup of lanthanide ions [96], the conformation inversion of the 18-crown-6 in the complexes of $[Ln(18\text{-crown-}6)(NO_3)_3]$ [202]}. As one can see from Table 11, the free energy values obtained in different ways differ in 5 kJ mol^{-1}(Yb), 7 kJ mol^{-1}(Pr) and 9 kJ mol^{-1}(Eu). Three different methods (^{1}H EXSY-CT, ^{17}O BSA and ^{1}H BSATTD-LIS) have been used in the experimental studies concerning the complexes (Table 12). Two of them are based on ^{1}H NMR data. The third method is based on ^{17}O NMR data. Using these methods to measure the energy parameters of molecular dynamics can lead to systematic errors [14]. Moreover, in some cases, a part of the data has been obtained for the case of aqueous solutions and the other part- for solutions in a water–methanol mixture [14]. All of these factors can lead to systematic errors in the assessment of the activation energy of conformational dynamics. These relatively large errors could be in particular caused by the necessity of correction for the temperature dependence of the paramagnetic LISs at the temperature range close to the coalescence. It has been found by ^{1}H NMR that the experimental LISs values (δ) of I, II and III are well fitted by linear dependence on $1/T$ (Fig. 19). In addition, in the case of DTPA complexes, the conformational dynamics parameters can depend also on the pH value of the solutions, since these complexes form acidic complexes (unlike, for example, DOTA).

Derivative $\delta(T)$ has been calculated for signals obtained from I, II and III in D_2O at 278 K, the maximum values thereof amounting to 0.17, 0.43 and 0.64 p.p.m./K for I, II and III respectively. It should be noted that other complex compounds, studied earlier using ^{1}H NMR both in organic and in aqueous media, are characterized by the LIS temperature sensitivity ranging from 0 to 1.5 p.p.m./K. The obtained results indicate that coordination compounds I, II and III could be considered as moderately sensitive ^{1}H NMR

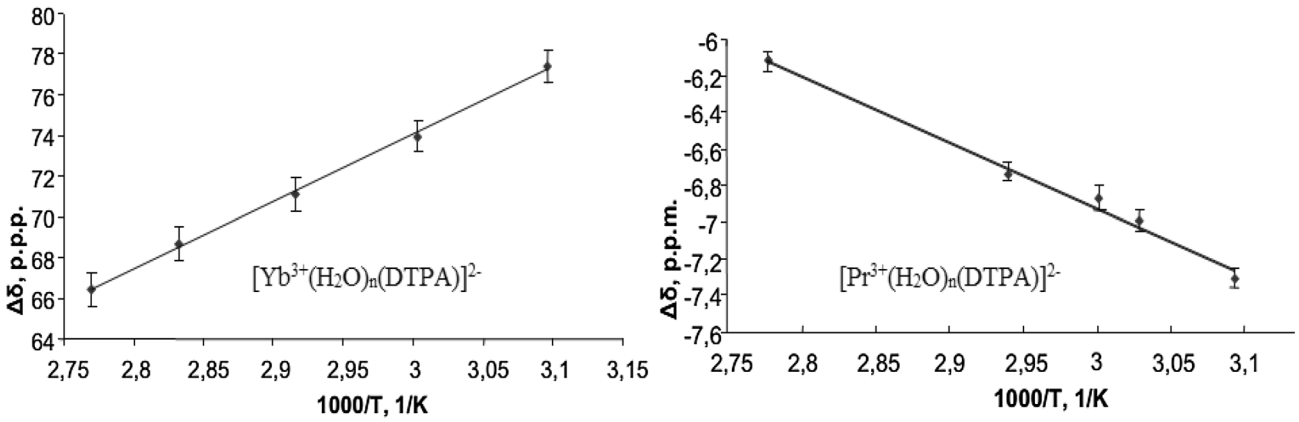

Fig. 19 Paramagnetic LISs in 500 MHz ^{1}H NMR of $[Yb^{3+}(H_2O)n(DTPA)]^{2-}$ and $[Pr^{3+}(H_2O)_n(DTPA)]^{2-}$ depending on $1/T$ at pH 7; concentration is 5×10^{-3} M in D_2O [207]

lanthanide paramagnetic probes for in situ temperature control in aqueous solution.

The temperature dependences of paramagnetic lanthanide induced shifts in NMR spectra show that Ln complexes with DTPA ligand could be of practical importance in medicine and biology as thermo-sensing MRI contrast agents for cancer and inflammation detection (via mapping the temperature distribution in a human or animal body).

Conclusions

In this review, we have shown how the NMR method can be used in the analysis of the molecular structure and dynamics of Ln complexes with PAPC ligands (EDTA, DOTA and DTPA and some of their derivatives).

We have carried out a detailed description of the methods available from the literature for studying the structure and molecular dynamics of lanthanide paramagnetic complexes in solutions. It is emphasized that the currently available NMR investigation methods make it possible to perform an efficient determination of the structure and molecular dynamics of kinetically stable dissolved lanthanide complexes with different organic complexing agents including EDTA-like, DTPA-like and DOTA-like ligands.

The analysis of pseudocontact contributions to the LISs provides, in particular, making it possible to determine structural parameters for Ln complexes.

Another completely independent approach to the studies on the structure of paramagnetic lanthanide complexes consists in the analysis of paramagnetic relaxation rate enhancement on the ligand nuclei. In this context, the following two efficient directions should be noted. They consist in the analysis of dipole contributions to paramagnetic relaxation rate enhancement, and in the studies on Curie-spin contributions to paramagnetic relaxation rate enhancement.

Paramagnetic lanthanide cations represent adjustable probes for studying dynamic processes occurring in substrate molecules that can form complexes with lanthanide cations in solution. The paramagnetic lanthanide probe provides an extension in the range of rate constant values for chemical exchange processes in comparison with DNMR application to diamagnetic substances. The following four dynamic NMR techniques are chosen to use not only for qualitative, but also for quantitative studies on the processes occurring in substrate molecules of lanthanide complexes: band-shape analysis taking into account lanthanide-induced chemical shifts (for Ce, Pr, Nd, Eu, Tb, Dy, Ho, Er, Tm, Yb) depending on temperature, selective magnetization transfer (for Eu), spin saturation transfer (for Pr and Dy), and 2D exchange spectroscopy (for Pr, Eu and Yb).

By using this set of methods, it has been found that free molecular-dynamics activation energy $\Delta G^{\neq}_{298}$ in the series of $Na_2[Ln(DTPA)(H_2O)]$, $Na[Ln(H_2O)(DOTA)]$, $Na[Yb(H_2O)(EDTA)]$, and $[Ln(18\text{-crown-}6)(NO_3)_3]$ complexes monotonously changes with decreasing lanthanide cation radius. This is most likely owing to the effect of lanthanide contraction.

According to the analysis of the data obtained for a large number of lanthanide complexes with different PAPC ligands, it can be concluded that LISs have a linear dependence on the inverse temperature ($1/T$).

It should be also noted that based on the mentioned features the Ln complexes exhibit sensory properties in determining local temperature in liquid organic and aqueous media, which has been verified using a considerable set of lanthanide complexes.

Recently, there have appeared some examples that demonstrate the potentialities of using such complexes, for example, as relaxation thermosensor probes.

The analysis of paramagnetic properties such as the temperature sensitivity of LIS and paramagnetic increases in relaxation rates indicates the prospect of using kinetically stable lanthanide complexes as shift and relaxation temperature-sensitive probes for determining local temperature and diagnosing diseases using MRI technologies. In general, NMR confirms its high efficiency as an analytical method and, in combination with contrast methods in MRI, shows new possibilities in the diagnosis of diseases (in particular in oncology).

Acknowledgements The research was supported by the Russian science foundation (the research project № 20-63-46026).

Declarations

Conflict of interest There are no conflicts to declare.

References

1. Sherry, A.D., Geraldes, C.F.G.C.: Lanthanide Probes in Life, Chemical and Earth Sciences. Elsevier, Amsterdam (1989)
2. Parker, D., Dickins, R.S., Puschmann, H., Crossland, C., Howard, J.A.K.: Being excited by lanthanide coordination complexes: aqua species, chirality, excited-state chemistry, and exchange dynamics. Chem. Rev. **102**, 1977–2010 (2002). https://doi.org/10.1021/cr010452+
3. Otting, G.: Protein NMR using paramagnetic ions. Annu. Rev. Biophys. **39**, 387–405 (2010). https://doi.org/10.1146/annurev.biophys.093008.131321
4. Riehemann, K., Schneider, S.W., Luger, T.A., Godin, B., Ferrari, M., Fuchs, H.: Nanomedicine - challenge and perspectives. Angew. Chem. Int. Ed. **48**, 872–897 (2009). https://doi.org/10.1002/anie.200802585
5. Godin, B., Sakamoto, J.H., Serda, R.E., Grattoni, A., Bouamrani, A., Ferrari, M.: Emerging applications of nanomedicine for the diagnosis and treatment of cardiovascular diseases. Trends

Pharmacol. Sci. **31**, 199–205 (2010). https://doi.org/10.1016/j.tips.2010.01.003
6. Voronov, V.K., Ushakov, I.A.: High-resolution nuclear magnetic resonance in paramagnetic complexes. Russ. Chem. Rev. **79**, 835–847 (2010). https://doi.org/10.1070/rc2010v079n10abeh004157
7. Piguet, C., Geraldes, C.F.G.C.: Handbook on the Physics and Chemistry of Rare Earths. Elsevier Science, Amsterdam (2003)
8. Babailov, S.P.: Lanthanide paramagnetic probes for NMR spectroscopic studies of molecular conformational dynamics in solution: applications to macrocyclic molecules. Prog. Nucl. Magn. Reson. Spectrosc. **52**, 1–21 (2008). https://doi.org/10.1016/j.pnmrs.2007.04.002
9. Gordon, J.W., Fain, S.B., Rowland, I.J.: Effect of lanthanide ions on dynamic nuclear polarization enhancement and liquid-state T1 relaxation. Magn. Reson. Med. **68**, 1949–1954 (2012). https://doi.org/10.1002/mrm.24207
10. Peat, D.T., Horsewill, A.J., Köckenberger, W., Linde, A.J.P., Gadian, D.G., Owers-Bradley, J.R.: Achievement of high nuclear spin polarization using lanthanides as low-temperature NMR relaxation agents. Phys. Chem. Chem. Phys. **15**, 7586–7591 (2013). https://doi.org/10.1039/c3cp00103b
11. Rigault, S., Piguet, C.: Predictions and assignments of NMR spectra for strongly paramagnetic supramolecular lanthanide complexes: the effect of the "gadolinium break." J. Am. Chem. Soc. **122**, 9304–9305 (2000). https://doi.org/10.1021/ja000958u
12. Viswanathan, S., Kovacs, Z., Green, K.N., Ratnakar, S.J., Sherry, A.D.: Alternatives to gadolinium-based metal chelates for magnetic resonance imaging. Chem. Rev. **110**, 2960–3018 (2010). https://doi.org/10.1021/cr900284a
13. Babailov, S.P.: Lanthanide paramagnetic probes for NMR spectroscopic studies of fast molecular conformational dynamics and temperature control. Effective six-site proton exchange in 18-crown-6 by exchange spectroscopy. Inorg. Chem. **51**, 1427–1433 (2012). https://doi.org/10.1021/ic201662q
14. Jenkins, B.G., Lauffer, R.B.: Solution structure and dynamics of lanthanide(III) complexes of diethylenetriaminepentaacetate: a two-dimensional NMR analysis. Inorg. Chem. **27**, 4730–4738 (1988). https://doi.org/10.1021/ic00299a011
15. Aime, S., Botta, M., Fasano, M., Terreno, E.: Lanthanide(in) chelates for NMR biomedical applications. Chem. Soc. Rev. **27**, 19–29 (1998). https://doi.org/10.1039/A827019Z
16. Ananta, J.S., Godin, B., Sethi, R., Moriggi, L., Liu, X., Serda, R.E., Krishnamurthy, R., Muthupillai, R., Bolskar, R.D., Helm, L., Ferrari, M., Wilson, L.J., Decuzzi, P.: Geometrical confinement of gadolinium-based contrast agents in nanoporous particles enhances T1 contrast. Nat. Nanotechnol. **5**, 815–821 (2010). https://doi.org/10.1038/nnano.2010.203
17. Della Rocca, J., Lin, W.: Nanoscale metal-organic frameworks: magnetic resonance imaging contrast agents and beyond. Eur. J. Inorg. Chem. (2010). https://doi.org/10.1002/ejic.201000496
18. Henriques, E.S., Geraldes, C.F.G.C., Ramos, M.J.: Modelling studies in aqueous solution of lanthanide (III) chelates designed for nuclear magnetic resonance biomedical applications. Mol. Phys. **101**, 2319–2333 (2003). https://doi.org/10.1080/00268970310001080023
19. Hingorani, D.V., Gonzalez, S.I., Li, J.F., Pagel, M.D.: Sensing lanthanide metal content in biological tissues with magnetic resonance spectroscopy. Sensors (Switzerland). **13**, 13732–13743 (2013). https://doi.org/10.3390/s131013732
20. Schühle, D.T., Van Rijn, P., Laurent, S., Vander Elst, L., Muller, R.N., Stuart, M.C.A., Schatz, J., P eters, J.A.: Liposomes with conjugates of a calix[4]arene and a Gd-DOTA derivative on the outside surface: an efficient potential contrast agent for MRI. Chem. Commun. **46**, 4399–4401 (2010). https://doi.org/10.1039/c0cc00107d
21. Caravan, P.: Strategies for increasing the sensitivity of gadolinium based MRI contrast agents. Chem. Soc. Rev. **35**, 512–523 (2006). https://doi.org/10.1039/b510982p
22. Caravan, P., Ellison, J.J., Mcmurry, T.J., Lauffer, R.B.: Gadolinium(III) chelates as MRI contrast agents: structure, dynamics, and applications. Chem. Rev. **99**, 2293–2352 (1999). https://doi.org/10.1021/cr980440x
23. Davidenko, N.K., Zinich, N.N.: Lanthanide-ion-induced paramagnetic shifts in NMR spectra in aqueous solutions. Theor. Exp. Chem. **12**, 552–554 (1977). https://doi.org/10.1007/BF00525185
24. Ryhl, T.: Kinetics studies of lanthanoid carboxylate complexes. II. A PMR investigation of the lanthanum and lutetium EDTA complexes. Acta Chem. Scand. **26**, 4001–4007 (1972). https://doi.org/10.3891/acta.chem.scand.26-4001
25. Peters, J.A., Huskens, J., Raber, D.J.: Lanthanide induced shifts and relaxation rate enhancements. Prog. Nucl. Magn. Reson. Spectrosc. **28**, 283–350 (1996). https://doi.org/10.1016/0079-6565(95)01026-2
26. Geraldes, C.F.G.C.: NMR in Supramolecular Chemistry. Kluwer, Netherlands (1999)
27. Evans, C.H.: Biochemistry of Lanthanides. Plenum, New York (1990)
28. Bertini, I., Luchinat, C.H.: Coordination Chemistry Reviews: NMR of Paramagnetic Substances. Elsevier, Amsterdam (1996)
29. Vonci, M., Mason, K., Suturina, E.A., Frawley, A.T., Worswick, S.G., Kuprov, I., Parker, D., McInnes, E.J.L., ChiltoN,N.F.: Rationalization of anomalous pseudocontact shifts and their solvent dependence in a series of C3-symmetric lanthanide complexes. J. Am. Chem. Soc. **139**, 14166–14172 (2017). https://doi.org/10.1021/jacs.7b07094
30. Golding, R.M., Pyykkö, P.: On the theory of pseudoeontact N.M.R. shifts due to lanthanide complexest. Mol. Phys. **26**, 1389–1396 (1973). https://doi.org/10.1080/00268977300102561
31. De Boer, J.W.M., Sakkers, P.J.D., Hilbers, C.W., De Boer, E.: Lanthanide shift reagents. II. Shift mechanisms. J. Magn. Reson. **25**, 455–476 (1977). https://doi.org/10.1016/0022-2364(77)90209-8
32. Rodríguez-Rodríguez, A., Esteban-Gómez, D., De Blas, A., Rodríguez-Blas, T., Botta, M., Tripier, R., Platas-Iglesias, C.: Solution structure of Ln(III) complexes with macrocyclic ligands through theoretical evaluation of 1H NMR contact shifts. Inorg. Chem. **51**, 13419–13429 (2012). https://doi.org/10.1021/ic302322r
33. Woods, M., Aime, S., Botta, M., Howard, J.A.K., Moloney, J.M., Navet, M., Parker, D., Port, M., Rousseaux, O.: Correlation of water exchange rate with isomeric composition in diastereoisomeric gadolinium complexes of tetra(carboxyethyl) dota and related macrocyclic ligands. J. Am. Chem. Soc. **122**, 9781–9792 (2000). https://doi.org/10.1021/ja994492v
34. Dunand, F.A., Dickins, R.S., Parker, D., Merbach, A.E.: Towards rational design of fast water-exchanging Gd(dota-like) contrast agents? Importance of the M/m ratio. Chem. A Eur. J. **7**, 5160–5167 (2001). https://doi.org/10.1002/1521-3765(20011203)7:23%3c5160::AID-CHEM5160%3e3.0.CO;2-2
35. S.P. Babailov, A.G. Coutsolelos, A. Dikiy, G.A. Spyroulias, Intramolecular dynamics of asymmetric lanthanide(III) porphyrin sandwich complexes in solution, Eur. J. Inorg. Chem. (2001). https://doi.org/10.1002/1099-0682(20011)2001:1<303::AID-EJIC303>3.0.CO;2-Y.
36. La Mar, G.N., Faller, J.W.: Strategies for the study of structure using lanthanide reagents. J. Am. Chem. Soc. **95**, 3817–3818 (1973). https://doi.org/10.1021/ja00792a071
37. Bertini, I., Coutsolelos, A., Dikiy, A., Luchinat, C., Spyroulias, G.A., Troganis, A., Capponi, G.: Structural and dynamic information on double-decker Yb3+ and Dy3+ porphyrin complexes

in solution through 1H NMR. Inorg. Chem. **35**, 6308–6315 (1996). https://doi.org/10.1021/ic960339f
38. Wenzel, T.G.: NMR Shift Reagents. CRC Press, Boca Raton (1987)
39. Bleaney, B.: Nuclear magnetic resonance shifts in solution due to lanthanide ions. J. Magn. Reson. **8**, 91–100 (1972). https://doi.org/10.1016/0022-2364(72)90027-3
40. Kemple, M.D., Ray, B.D., Lipkowitz, K.B., Prendergast, F.G., Rao, B.D.N.: The use of lanthanides for solution structure determination of biomolecules by NMR. Evaluation of the methodology with EDTA derivatives as model systems. J. Am. Chem. Soc. **110**, 8275–8287 (1988). https://doi.org/10.1021/ja00233a001
41. Nadaud, P.S., Helmus, J.J., Kall, S.L., Jaroniec, C.P.: Paramagnetic ions enable tuning of nuclear relaxation rates and provide long-range structural restraints in solid-state NMR of proteins. J. Am. Chem. Soc. (2009). https://doi.org/10.1021/ja900224z
42. Schultz, P.G., Dervan, P.B.: Sequence-specific double-strand cleavage of DNA by penta-N-methylpyrrolecarboxamide-EDTA·Fe(II). Proc. Natl. Acad. Sci. USA **80**, 6834–6837 (1983). https://doi.org/10.1073/pnas.80.22.6834
43. Peters, J.A.: Analysis of multinuclear lanthanide-induced shifts. 4. Some consequences of the lanthanide contraction. J. Magn. Reson. **68**, 240–251 (1986). https://doi.org/10.1016/0022-2364(86)90241-6
44. Koehler, J., Meiler, J.: Expanding the utility of NMR restraints with paramagnetic compounds: background and practical aspects. Prog. Nucl. Magn. Reson. Spectrosc. **59**, 360–389 (2011). https://doi.org/10.1016/j.pnmrs.2011.05.001
45. Suturina, E.A., Mason, K., Geraldes, C.F.G.C., ChiltoN,N.F., Parker, D., Kuprov, I.: Lanthanide-induced relaxation anisotropy. Phys. Chem. Chem. Phys. **20**, 17676–17686 (2018). https://doi.org/10.1039/c8cp01332b
46. Derendyaev, B.G., Mamatyuk, V.I., Koptyug, V.A.: The labelling via saturation of a spin system in study of mechanisms of moderatelly rapid reversible reactions - an example. Tetrahed Lett. (1969). https://doi.org/10.1016/S0040-4039(01)97637-3
47. Spyroulias, G.A., Coutsolelos, A.G.: Evidence of Protonated and Deprotonated Forms of Symmetrical and Asymmetrical Lutetium(III) Porphyrin Double-Deckers by 1H-NMR Spectroscopy. Inorg. Chem. **35**, 1382–1385 (1996). https://doi.org/10.1021/ic950796g
48. Babailov, S.P., Kruppa, A.I., Glebov, E.M., Plyusnin, V.F.: NMR in photo-induced chemical exchange systems. Double-resonance inverse fractional population transfer application for investigation of 1,2-(2,2′-dipyridyl)ethene photoisomerization kinetics. Concepts Magn. Reson. Part A Bridg. Educ. Res. **28**, 337–346 (2006). https://doi.org/10.1002/cmr.a.20063
49. Grant, C.V., Sit, S.L., De Angelis, A.A., Khuong, K.S., Wu, C.H., Plesniak, L.A., Opella, S.J.: An efficient 1H/31P double-resonance solid-state NMR probe that utilizes a scroll coil. J. Magn. Reson. **188**, 279–284 (2007). https://doi.org/10.1016/j.jmr.2007.06.016
50. Damjanovic, M., Katoh, K., Yamashita, M., Enders, M.: Combined NMR analysis of huge residual dipolar couplings and pseudocontact shifts in terbium(III)-phthalocyaninato single molecule magnets. J. Am. Chem. Soc. **135**, 14349–14358 (2013). https://doi.org/10.1021/ja4069485
51. Allegrozzi, M., Bertini, I., Janik, M.B.L., Lee, Y.M., Liu, G., Luchinat, C.: Lanthanide-induced pseudocontact shifts for solution structure refinements of macromolecules in shells up to 40 Å from the metal ion. J. Am. Chem. Soc. **122**, 4154–4161 (2000). https://doi.org/10.1021/ja993691b
52. Babailov, S.P., Zapolotsky, E.N.: A new approach to determining the structure of lanthanide complexes in solution according to the Curie-spin contribution to the paramagnetic spin-spin relaxation rate enhancements : Ho-DOTA. Polyhedron **182**, 114487 (2020). https://doi.org/10.1016/j.poly.2020.114487
53. Wang, F., Shao, N., Cheng, Y.: Paramagnetic NMR investigation of dendrimer-based host-guest interactions. PLoS ONE **8**, 2–9 (2013). https://doi.org/10.1371/journal.pone.0064722
54. Erasmus, C.S., Boeyens, J.C.A.: Crystal structure of the praseodymium β-diketonate of 2,2,6,6-tetramethyl-3,5-heptanedione, Pr 2 (thd) 6. Acta Crystallogr Sect. B Struct. Crystallogr. Cryst. Chem. **26**, 1843–1854 (1970). https://doi.org/10.1107/s0567740870004983
55. de Villiers, J.P.R., Boeyens, J.C.A.: The crystal and molecular structure of the hydrated praseodymium chelate of 1,1,1,2,2,3,3-heptafluoro-7,7-dimethyl-4,6-octanedione, Pr2(fod)6.2H_2O. Acta Crystallogr Sect. B Struct. Crystallogr. Cryst. Chem. **27**, 692–702 (1971). https://doi.org/10.1107/s0567740871002784
56. Renaud, F., Piguet, C., Bernardinelli, G., Bünzli, J.C.G., Hopfgartner, G.: In search for mononuclear helical lanthanide building blocks with predetermined properties: triple-stranded helical complexes with N,N, N', N'-tetraethylpyridine-2,6-dicarboxamide. Chem. A Eur. J. **3**, 1646–1659 (1997). https://doi.org/10.1002/chem.19970031014
57. Forsberg, J.H., Delaney, R.M., Zhao, Q., Harakas, G., Chandran, R.: Analyzing lanthanide-induced shifts in the NMR spectra of lanthanide(III) complexes derived from 1,4,7,10-tetrakis(N,N-diethylacetamido)-1,4,7,10-tetraazacyclododecane. Inorg. Chem. **34**, 3705–3715 (1995). https://doi.org/10.1021/ic00118a018
58. Banci, L., Bertini, I., Cavallaro, G., Giachetti, A., Luchinat, C., Parigi, G.: Paramagnetism-based restraints for Xplor-NIH. J. Biomol. NMR. **28**, 249–261 (2004). https://doi.org/10.1023/B:JNMR.0000013703.30623.f7
59. Clore, G.M., Iwahara, J.: Theory, practice, and applications of paramagnetic relaxation enhancement for the characterization of transient low-population states of biological macromolecules and their complexes G. Chem. Rev. **109**, 4108–4139 (2009). https://doi.org/10.1021/cr900033p
60. Aime, S., Botta, M., Fasano, M., Marques, M.P.M., Geraldes, C.F.G.C., Pubanz, D., Merbach, A.E.: Conformational and coordination equilibria on DOTA complexes of lanthanide metal ions in aqueous solution studied by 1H-NMR spectroscopy. Inorg. Chem. **36**, 2059–2068 (1997). https://doi.org/10.1021/ic961364o
61. Panich, A.M., Salti, M., Goren, S.D., Yudina, E.B., Aleksenskii, A.E., Vul, A.Y., Shames, A.I.: Gd(III)-grafted detonation nanodiamonds for MRI contrast enhancement. J. Phys. Chem. C. **123**, 2627–2631 (2019). https://doi.org/10.1021/acs.jpcc.8b11655
62. Medina, D.C., Springer, J.C.S.: T2-Selective MRI contrast-reagents: revisiting the inner-sphere curie-spin relaxation mechanism of dysprosium(III) chelates. Proc Intl Soc Mag Reson Med. **11**, 816 (2003)
63. Vander Elst, L., Roch, A., Gillis, P., Laurent, S., Botteman, F., Bulte, J.W.M., Muller, R.N.: Dy-DTPA derivatives as relaxation agents for very high field MRI: the beneficial effect of slow water exchange on the transverse relaxivities. Magn. Reson. Med. **47**, 1121–1130 (2002). https://doi.org/10.1002/mrm.10163
64. Caravan, P., Greenfield, M.T., Bulte, J.W.M.: Molecular factors that determine curie spin relaxation in dysprosium complexes. Magn. Reson. Med. **922**, 917–922 (2001). https://doi.org/10.1002/mrm.1277
65. Babailov, S.P., Zapolotsky, E.N., Basova, T.V.: Holmium-DOTA as a responsive relaxation paramagnetic probe for NMR/MRI control of local temperature at high magnetic fields. Inorg. Chim. Acta. **493**, 57–60 (2019). https://doi.org/10.1016/j.ica.2019.04.003
66. Babailov, S.P., Polovkova, M.A., Kirakosyan, G.A., Martynov, A.G., Zapolotsky, E.N., Gorbunova, Y.G.: NMR thermosensing

properties on binuclear triple-decker complexes of terbium(III) and dysprosium(III) with 15-crown-5-phthalocyanine. Sens. Actuators A Phys. **331**, 112933 (2021). https://doi.org/10.1016/j.sna.2021.112933
67. Babailov, S.P., Zapolotsky, E.N.: Dy-DTPA as supersensitive shifting and relaxational probe for NMR/MRI control of local temperature. Polyhedron **194**, 114908 (2021). https://doi.org/10.1016/j.poly.2020.114908
68. S.P. Babailov, E.N. Zapolotsky, Dy-DOTA complex as promising shifting and relaxational NMR thermo-sensor probe, Inorg. Chim. Acta. (2021).
69. Babailov, S.P., Dubovskii, P.V., Zapolotsky, E.N.: Paramagnetic lanthanides as magnetic resonance thermo-sensors and probes of molecular dynamics : holmium-DOTA complex. Polyhedron **79**, 277–283 (2014). https://doi.org/10.1016/j.poly.2014.04.067
70. Aime, S., Botta, M., Ermondi, G.: NMR study of solution structures and dynamics of lanthanide(III) complexes of DOTA. Inorg. Chem. **31**, 4291–4299 (1992). https://doi.org/10.1021/ic00047a016
71. Dunand, F.A., Aime, S., Merbach, A.E.: First 17O NMR observation of coordinated water on both isomers of [Eu(DOTAM)(H_2O)]$^{3+}$: a direct access to water exchange and its role in the isomerization. J. Am. Chem. Soc. **122**, 1506–1512 (2000). https://doi.org/10.1021/ja993204s
72. Sandstrom, J.: Dynamic NMR Spectroscopy. Acad. Press, London (1982)
73. Schneider, H.J., Freitag, W., Schommer, M.: A chemical shift 1CMR thermometer: The TMS 13C shift dependence on absolute temperature. J. Magn. Reson. **18**, 393–395 (1975). https://doi.org/10.1016/0022-2364(75)90139-0
74. Stout, E.W., Gutowsky, H.S.: On the temperature dependence of lanthanide-induced NMR shifts. J. Magn. Reson. **398**, 389–398 (1976). https://doi.org/10.1016/0022-2364(76)90118-9]
75. Cheng, H.N., Gutowsky, H.S.: Temperature dependence of lanthanide induced chemical shifts. J. Phys. Chem. **82**, 914–921 (1978). https://doi.org/10.1021/j100497a015
76. T.A. Babushkina, V.F. Zolin, L.G. Koreneva, Interpretation of lanthanide-induced shifts in NMR spectra. The case of nonaxial symmetry, J. Magn. Reson. 52 (1983) 169–181. https://doi.org/10.1016/0022-2364(83)90185-3.
77. Selyutina, O.Y., Kononova, P.A., Babailov, S.P.: Complex of praseodymium with lipid as a NMR temperature sensor and probe of liposome states. New J. Chem. **44**, 18372–18379 (2020). https://doi.org/10.1039/d0nj03707a
78. De Poorter, J., De Wagter, C., De Deene, Y., Thomsen, C., Ståhlberg, F., Achten, E.: Noninvasive MRI Thermometry with the Proton Resonance Frequency (PRF) method: in vivo results in human muscle. Magn. Reson. Med. **33**, 74–81 (1995). https://doi.org/10.1002/mrm.1910330111
79. Frenzel, T., Roth, K., Koßler, S., Radüchel, B., Bauer, H., Platzek, J., Weinmann, H.J.: Noninvasive temperature measurement in vivo using a temperature-sensitive lanthanide complex and 1H magnetic resonance spectroscopy. Magn. Reson. Med. **35**, 364–369 (1996). https://doi.org/10.1002/mrm.1910350314
80. Bertsch, F., Mattner, J., Stehling, M.K., Müller-Lisse, U., Peller, M., Loeffler, R., Weber, J., Meßmer, K., Wilmanns, W., Issels, R., Reiser, M.: Non-invasive temperature mapping using MRI: comparison of two methods based on chemical shift and T1-relaxation. Magn. Reson. Imaging. **16**, 393–403 (1998). https://doi.org/10.1016/S0730-725X(97)00311-1
81. Zuo, C.S., Bowers, J.L., Metz, K.R., Nosaka, T., Sherry, A.D., Clouse, M.E.: TmDOTP5-: a substance for NMR temperature measurements in vivo. Magn. Reson. Med. **36**, 955–959 (1996). https://doi.org/10.1002/mrm.1910360619
82. Zuo, C.S., Metz, K.R., Sun, Y., Sherry, A.D.: NMR temperature measurements using a paramagnetic lanthanide complex. J. Magn. Reson. **133**, 53–60 (1998). https://doi.org/10.1006/jmre.1998.1429
83. Sun, Y., Sugawara, M., Mulkern, R.V., Hynynen, K., Mochizuki, S., Albert, M., Zuo, C.S.: Simultaneous measurements of temperature and pH in vivo using NMR in conjunction with TmDOTP5-. NMR Biomed. **13**, 460–466 (2000). https://doi.org/10.1002/nbm.676
84. Hekmatyar, S.K., Poptani, H., Babsky, A., Leeper, D.B., Bansal, N.: Non-invasive magnetic resonance thermometry using thulium-1,4,7,10-tetraazacyclododecane-1,4,7,10-tetraacetate (TmDOTA). Int J Hyperth. **18**, 165–179 (2002). https://doi.org/10.1080/02656730110098598
85. Trübel, H.K.F., Maciejewski, P.K., Farber, J.H., Hyder, F.: Brain temperature measured by 1H-NMR in conjunction with a lanthanide complex. J. Appl. Physiol. **94**, 1641–1649 (2003). https://doi.org/10.1152/japplphysiol.00841.2002
86. Pakin, S.K., Hekmatyar, S.K., Hopewell, P., Babsky, A., Bansal, N.: Non-invasive temperature imaging with thulium 1,4,7,10-tetraazacyclododecane-1,4,7, 10-tetramethyl-1,4,7,10-tetraacetic acid (TmDOTMA-). NMR Biomed. **19**, 116–124 (2006). https://doi.org/10.1002/nbm.1010
87. Coman, D., Trubel, H.K., Hyder, F.: Brain temperature by Biosensor Imaging of Redundant Deviation in Shifts (BIRDS): comparison between TmDOTP5− and TmDOTMA. NMR Biomed. **2010**(23), 277–285 (2010). https://doi.org/10.1002/nbm.1461.Brain
88. Chisolm, J.J.: BAL, EDTA, DMSA and DMPS in the treatment of lead poisoning in children. Clin. Toxicol. **30**, 493–504 (1992). https://doi.org/10.3109/15563659209017937
89. Dyatlova, N.M., Temkina, V.Y., Popov, K.I.: Complexons and Complexonates of Metals. Chemistry, Moscow (1988)
90. Janicki, R., Mondry, A.: A new approach to determination of hydration equilibria constants for the case of [Er(EDTA)(H_2O)n]-complexes. Phys. Chem. Chem. Phys. **16**, 26823–26831 (2014). https://doi.org/10.1039/c4cp04093g
91. Maigut, J., Meier, R., Zahl, A., Van Eldik, R.: Effect of chelate dynamics on water exchange reactions of paramagnetic aminopolycarboxylate complexes. Inorg. Chem. **47**, 5702–5719 (2008). https://doi.org/10.1021/ic702421z
92. Yong, B., Han, S., Ni, L., Su, T., Garcia, A.: Dynamic NMR of intramolecular exchange processes in EDTA complexes Sc3+, Y3+, and La3+. J. Chem. Educ. **83**, 296–298 (2006). https://doi.org/10.1021/ed083p296
93. Ryhl, T.: Kinetic studies of lanthanoid carboxylate complexes III The dissociation rates of praseodymium, neodymium, europium, and erbium EDTA complexes. Acta Chem. Scand. **27**, 303–314 (1973). https://doi.org/10.3891/acta.chem.scand.27-030
94. Babailov, S.P.: Subnanosize thermometric NMR sensors based on paramagnetic lanthanide(III) complexes with EDTA for temperature control in aqueous media and in magnetoresonance tomography. Russ. Chem. Bull. **6**, 1292–1293 (2008). https://doi.org/10.1007/s11172-008-0170-0
95. Babailov, S.P., Kokovkin, V.V., Stabnikov, P.A.: Paramagnetic properties and complexation kinetics of edta with praseodymium and holmium(III) cations in aqueous solution. J. Struct. Chem. **51**, 682–686 (2010). https://doi.org/10.1007/s10947-010-0095-y
96. Babailov, S.P.: Intermolecular dynamics and paramagnetic properties of ethylenediaminetetraacetate complexes with the yttrium subgroup rare earth elements using nuclear magnetic resonance. Magn. Reson. Chem. **50**, 793–797 (2012). https://doi.org/10.1002/mrc.3884
97. Gennaro, M.C., Mirti, P., Casalino, C.: NMR study of intramolecular processes in EDTA metal complexes. Polyhedron **2**, 13–18 (1983). https://doi.org/10.1016/S0277-5387(00)88025-0

98. Babailov, S.P., Chuikov, I.P., Kruppa, A.I.: Activation energies of intermolecular dynamics in ethylenediaminetetraacetate complexes with lanthanides: an effect of the "gadolinium break." Inorganica Chim. Acta. **439**, 117–122 (2016). https://doi.org/10.1016/j.ica.2015.10.009
99. Babailov, S.P.: Paramagnetic NMR: molecular structure and chemical exchange processes in d- and f-element coordination compounds in solution. LAP Lambert Academic Publishing, New York. (2012)
100. Southwood-Jones, R.V.S., Merbach, A.E.: Nuclear magnetic resonance study of praseodymium, europium and ytterbium ethylenediaminetetraacetates. Inorg. Chim. Acta. **30**, 77–82 (1978). https://doi.org/10.1016/S0020-1693(00)89018-0
101. Brücher, E., Király, R., Nagypál, I.: Equilibrium relations of rare earth ethylene-diaminetetraacetate complexes in the presence of a ligand excess. J. Inorg. Nucl. Chem. **37**, 1009–1012 (1975). https://doi.org/10.1016/0022-1902(75)80688-9
102. Babailov, S.P., Stabnikov, P.A., Zapolotsky, E.N., Kokovkin, V.V.: Lanthanides as NMR probes of fast molecular dynamics at high magnetic fields and temperature sensors: conformational interconversion of erbium ethylenediaminetetraacetate complexes. Inorg. Chem. **52**, 5564–5569 (2013). https://doi.org/10.1021/ic400525r
103. Aime, S., Barge, A., Botta, M., Fasano, M., Ayala, J.D., Bombieri, G.: Crystal structure and solution dynamics of the lutetium(III) chelate of DOTA. Inorganica Chim. Acta. **246**, 423–429 (1996). https://doi.org/10.1016/0020-1693(96)05130-4
104. Babailov, S.P., Zapolotsky, E.N.: Complex of ytterbium ethylenediaminetetraacetate as combined NMR paramagnetic probe for in situ control of temperature and pH in aqueous media. Polyhedron **139**, 323–326 (2018). https://doi.org/10.1016/j.poly.2017.11.007
105. Koenig, S.H., Brown, R.D.: Field-cycling relaxometry of protein solutions and tissue. Implications for MRI. Prog. Nucl. Magn. Reson. Spectrosc. **22**, 487–567 (1990). https://doi.org/10.1016/0079-6565(90)80008-6
106. Kumar, K., Tweedle, M.F.: Macrocyclic polyaminocarboxylate complexes of lanthanides as magnetic resonance imaging contrast agents. Pure Appl. Chem. **65**, 515–520 (1993). https://doi.org/10.1351/pac199365030515
107. Bénazeth, S., Purans, J., Chalbot, M.C., Nguyen-Van-Duong, M.K., Nicolas, L., Keller, F., Gaudemer, A.: Temperature and pH dependence XAFS study of Gd(DOTA)- and $Gd(DTPA)_2$-complexes: solid state and solution structures. Inorg. Chem. **37**, 3667–3674 (1998). https://doi.org/10.1021/ic9707321
108. Lebduková, P., Hermann, P., Helm, L., Tóth, É., Kotek, J., Binnemans, K., Rudovský, J., Luke, I., Merbach, A.E.: Gadolinium(iii) complexes of mono- and diethyl esters of monophosphonic acid analogue of DOTA as potential MRI contrast agents: solution structures and relaxometric studies. Dalton Trans. (2007). https://doi.org/10.1039/b612876a
109. Micskei, K., Helm, L., Brucher, E., Merbach, A.E.: Oxygen-17 NMR study of water exchange on gadolinium polyaminopolyacetates $[Gd(DTPA)(H_2O)]_2$- and $[Gd(DOTA)(H_2O)]$-related to NMR imaging. Inorg. Chem. **32**, 3844–3850 (1993). https://doi.org/10.1021/ic00070a013
110. Aime, S., Botta, M., Garda, Z., Kucera, B.E., Tircso, G., Young, V.G., Woods, M.: Properties, solution state behavior, and crystal structures of chelates of DOTMA. Inorg. Chem. **50**, 7955–7965 (2011). https://doi.org/10.1021/ic2012827
111. Woods, M., Payne, K.M., Valente, E.J., Kucera, B.E., Young, V.G.: Crystal structures of DOTMA chelates from Ce3+ to Yb3+ : evidence for a continuum of metal Ion hydration states. Chem. A Eur. J. **25**, 9997–10005 (2019). https://doi.org/10.1002/chem.201902068
112. Rudovský, J., Botta, M., Hermann, P., Koridze, A., Aime, S.: Relaxometric and solution NMR structural studies on ditopic lanthanide(iii) complexes of a phosphinate analogue of DOTA with a fast rate of water exchange. Dalton Trans. (2006). https://doi.org/10.1039/b518147j
113. Joss, D., Häussinger, D.: Design and applications of lanthanide chelating tags for pseudocontact shift NMR spectroscopy with biomacromolecules. Prog. Nucl. Magn. Reson. Spectrosc. **114–115**, 284–312 (2019). https://doi.org/10.1016/j.pnmrs.2019.08.002
114. Pujales-Paradela, R., Savić, T., Pérez-Lourido, P., Esteban-Gómez, D., Angelovski, G., Botta, M., Platas-Iglesias, C.: Lanthanide complexes with 1 H paraCEST and 19 F response for magnetic resonance imaging applications. Inorg. Chem. **58**, 7571–7583 (2019). https://doi.org/10.1021/acs.inorgchem.9b00869
115. Mayer, F., Platas-Iglesias, C., Helm, L., Peters, J.A., Djanashvili, K.: 17O NMR and density functional theory study of the dynamics of the carboxylate groups in DOTA complexes of lanthanides in aqueous solution. Inorg. Chem. **51**, 170–178 (2012). https://doi.org/10.1021/ic201393n
116. Delgado, R., Félix, V., Lima, L.M.P., Price, D.W.: Metal complexes of cyclen and cyclam derivatives useful for medical applications: a discussion based on thermodynamic stability constants and structural data. Dalton Trans. (2007). https://doi.org/10.1039/b704360k
117. Zhang, S., Wu, K., Sherry, A.D.: Unusually sharp dependence of water exchange rate versus lanthanide ionic radii for a series of tetraamide complexes. J. Am. Chem. Soc. **124**, 4226–4227 (2002). https://doi.org/10.1021/ja017133k
118. Vipond, J., Woods, M., Zhao, P., Tircsó, G., Ren, J., Bott, S.G., Ogrin, D., Kiefer, G.E., Kovacs, Z., Sherry, A.D.: A bridge to coordination isomer selection in lanthanide(III) DOTA-tetraamide complexes. Inorg. Chem. **46**, 2584–2595 (2007). https://doi.org/10.1021/ic062184+
119. Jacques, V., Desreux, J.F.: Quantitative two-dimensional EXSY spectroscopy and dynamic behavior. Inorg. Chem. (1994). https://doi.org/10.1021/ic00096a033
120. Ratnakar, S.J., Chirayil, S., Funk, A.M., Zhang, S., Queiró, J.F., Geraldes, C.F.G.C., Kovacs, Z., Sherry, A.D.: A frequency-selective pH-responsive paraCEST agent. Angew. Chem. Int. Ed. **59**, 21671–21676 (2020). https://doi.org/10.1002/anie.202008888
121. Chang, C.A., Liu, Y.L., Chen, C.Y., Chou, X.M.: Ligand preorganization in metal ion complexation. Molecular mechanics/dynamics, kinetics, and laser-excited luminescence studies of trivalent lanthanide complex formation with macrocyclic ligands TETA and DOTA. Inorg. Chem. **40**, 3448–3455 (2001). https://doi.org/10.1021/ic001325j
122. Aime, S., Barge, A., Botta, M., De Sousa, A.S., Parker, D.: Direkter NMR-spektroskopischer Nachweis eines Lanthanoid-koordinierten Wassermoleküls, dessen Austauschgeschwindigkeit von der Konfiguration des Komplexes abhäng. Angew Chem. **110**, 2819–2820 (1998). https://doi.org/10.1002/(SICI)1521-3757(19981002)110:19%3c2819::AID-ANGE2819%3e3.0.CO;2-7
123. Polášek, M., Kotek, J., Hermann, P., Císařová, I., Binnemans, K., Lukeš, I.: Lanthanide(lll) complexes of pyridine-AKxide analogues of DOTA in solution and in the solid state. A new kind of isomerism in complexes of DOTA-like ligands. Inorg. Chem. **48**, 466–475 (2009). https://doi.org/10.1021/ic801597z
124. Mani, T., Tircsó, G., Togao, O., Zhao, P., Soesbe, T.C., Takahashi, M., Sherry, A.D.: Modulation of water exchange in Eu(III) DOTA-tetraamide complexes: considerations for in vivo imaging of PARACEST agents. Contrast Media Mol. Imaging. **4**, 183–191 (2009). https://doi.org/10.1002/cmmi.279

125. Green, K.N., Viswanathan, S., Rojas-Quijano, F.A., Kovacs, Z., Sherry, A.D.: Europium(III) DOTA-derivatives having ketone donor pendant arms display dramatically slower water exchange. Inorg. Chem. **50**, 1648–1655 (2011). https://doi.org/10.1021/ic101856d
126. Hoeft, S., Roth, K.: Struktur und Dynamik von Lanthanoid-Tetraazacyclododecantetraacetat-(DOTA-)Komplexen in Lösung. Chem. Ber. **126**, 869–873 (1993). https://doi.org/10.1002/cber.19931260404
127. Szilágyi, E., Tóth, É., Brücher, E., Merbach, A.E.: Lanthanide(III)–1,4,7,10-tetraazacyclododecane-1,4,7,10-tetraacetic acid complexes in acidic medium: significant decrease in water exchange rate, J Chem Soc. Dalton Trans. (1999). https://doi.org/10.1039/A903379C
128. Babailov, S.P., Nikulina, L.D., Krieger, J.H.: Intramolecular dynamics of lanthanide(III) tetraoxadiaza macrocycle complexes in solution as studied by NMR. J. Incl. Phenom. **43**, 25–29 (2002). https://doi.org/10.1023/A:1020492027829
129. Babailov, S.P., Mainichev, D.A., Nikulina, L.D., Petrova, S.S.: Intramolecular dynamics and molecular structure of europium(III) chelate complexes with crown ethers as studied by NMR spectroscopy. J. Incl. Phenom. Macrocycl. Chem. **51**, 73–78 (2005). https://doi.org/10.1007/s10847-004-2385-5
130. Babailov, S.P., Krieger, Y.G., Gabuda, S.P.: 1H NMR study of thedynamic structure of nitrate complexes of lanthanides with18-crown-6. Izv. Akad. Nauk SSSR. Ser. Khim. **11**, 2661–2662 (1990)
131. Babailov, S.P., Mainichev, D.A.: NMR studies of mixed-ligand lanthanide (III) complexes. Peculiarities of molecular structure, dynamics and paramagnetic properties for cerium subgroup chelates with crown ethers. J. Incl. Phenom. **43**, 187–194 (2002). https://doi.org/10.1023/A:1021237718495
132. Desreux, J.F.: Nuclear magnetic resonance spectroscopy of lanthanide complexes with a tetraacetic tetraaza macrocycle. Unusual conformation properties. Inorg Chem. **19**, 1319–1324 (1980). https://doi.org/10.1021/ic50207a042
133. Babailov, S.P., Zapolotsky, E.N., Kruppa, A.I., Stabnikov, P.A., Godovikov, I.A., Bocharov, E.V., Fomin, E.S.: Two types of conformational dynamics and thermo-sensor properties of praseodymium-DOTA by 1H/13C NMR. Inorg. Chim. Acta. **486**, 340–344 (2019). https://doi.org/10.1016/j.ica.2018.10.044
134. Blahut, J., Hermann, P., Tošner, Z., Platas-Iglesias, C.: A combined NMR and DFT study of conformational dynamics in lanthanide complexes of macrocyclic DOTA-like ligands. Phys. Chem. Chem. Phys. **19**, 26662–26671 (2017). https://doi.org/10.1039/c7cp05296k
135. Babailov, S.P., Krieger, Y.G.: NMR methods for molecular structure studies of paramagnetic lanthanide complexes in solutions. Applications to crown ether complexes. J. Struct. Chem. **39**, 580–593 (1998). https://doi.org/10.1007/BF02903634
136. Morrow, J.R., Amin, S., Lake, C.H., Churchill, M.R.: Synthesis, structure, and dynamic properties of the lanthanum(III) complex of 1,4,7,10-tetrakis(2-carbamoylethyl)-1,4,7,10-tetraazacyclododecane. Inorg Chem. **32**, 4566–4572 (1993). https://doi.org/10.1021/ic00073a017
137. Mani, F., Morassi, R., Stoppioni, P., Vacca, A.: Synthesis and kinetic behaviour of lanthanide(III) complexes with the mixed pendant-arm macrocyclic ligand 1,7-bis(carboxymethyl)-4,10-bis(1-methylimidazol-2-ylmethyl)-1,4,7, 10-tetraazacyclododecane. J. Chem. Soc. Dalton Trans. (2001). https://doi.org/10.1039/b101874o
138. Catton, G.A., Harman, M.E., Hart, F.A.: Complexes of lanthanoid salts with the crown ether cis, syn, cis-2,5,8,15,18,21-hexaoxatricyclo[20.4.0.0]hexacosane and their paramagnetically shifted nuclear magnetic resonance spectra. J. Chem. Soc. Dalton Trans. (1978). https://doi.org/10.1039/DT9780000181
139. Babailov, S.P., Zapolotsky, E.N., Fomin, E.S., Qu, Y.: Molecular structure and paramagnetic properties of bis-diisobutyldithiophosphinate complexes of europium(III), ytterbium(III) and lutetium(III) with 2,2-bipyridyl using NMR. Polyhedron **134**, 316–318 (2017). https://doi.org/10.1016/j.poly.2017.05.047
140. Desreux, J.F., Duyckaerts, G.: Sandwich macrocycle-lanthanide adducts with 12-crown-4. Synthesis and NMR study. Inorg Chim Acta. **35**, L313–L315 (1979). https://doi.org/10.1016/S0020-1693(00)93379-6
141. Desreux, J.F., Renard, A., Duyckaerts, G.: Complexes of lanthanide(III) nitrates with a tetraoxadiaza macrocycle. J. Inorg. Nucl. Chem. **39**, 1587–1591 (1977). https://doi.org/10.1016/0022-1902(77)80107-3
142. Babailov, S.P., Nikulina, L.D.: NMR studies of mixed-ligand lanthanide complexes in solution. Pseudorotation and ring inversion of 18-crown-6 molecule in cerium subgroup chelates. J. Incl. Phenom. **51**, 103–109 (2005). https://doi.org/10.1007/s10847-004-4673-5
143. Tashiro, K., Konishi, K., Aida, T.: Enantiomeric resolution of chiral metallobis(porphyrin)s: studies on rotatability of electronically coupled porphyrin ligands. Angew. Chem. **36**, 856–858 (1997). https://doi.org/10.1002/anie.199708561
144. Choppin, G.R.: A half-century of lanthanide aminopolycarboxylates. J. Alloys Compd. **192**, 256–261 (1993). https://doi.org/10.1016/0925-8388(93)90243-G
145. Repo, E., Warchoł, J.K., Bhatnagar, A., Mudhoo, A., Sillanpää, M.: Aminopolycarboxylic acid functionalized adsorbents for heavy metals removal from water. Water Res. **47**, 4812–4832 (2013). https://doi.org/10.1016/j.watres.2013.06.020
146. Arwidsson, Z., Elgh-Dalgren, K., von Kronhelm, T., Sjöberg, R., Allard, B., van Hees, P.: Remediation of heavy metal contaminated soil washing residues with amino polycarboxylic acids. J. Hazard. Mater. **173**, 697–704 (2010). https://doi.org/10.1016/j.jhazmat.2009.08.141
147. Runge, V.M., Clanton, J.A., Lukehart, C.M., Partain, C.L., James, J.E.A.: Paramagnetic agents for NMR imaging : a review. Am J Roentgenol. **141**, 1209–1215 (1983). https://doi.org/10.2214/ajr.141.6.1209
148. Smith, R.M., Martell, A.E.: Critical stability constants, enthalpies and entropies for the formation of metal complexes of aminopolycarboxylic acids and carboxylic acids. Sci. Total Environ. **64**, 125–147 (1987). https://doi.org/10.1016/0048-9697(87)90127-6
149. Hancock, R.D., Martell, A.E.: Ligand design for selective complexation of metal ions in aqueous solution. Chem. Rev. **89**, 1875–1914 (1989). https://doi.org/10.1021/cr00098a011
150. Hermann, P., Kotek, J., Kubíček, V., Lukeš, I.: Gadolinium(III) complexes as MRI contrast agents. Ligand design and properties of the complexes. Dalton Trans. **9226**, 3027–3047 (2008). https://doi.org/10.1039/b719704g
151. Pinto, I.S.S., Neto, I.F.F., Soares, H.M.V.M.: Biodegradable chelating agents for industrial, domestic, and agricultural applications—a review. Environ. Sci. Pollut. Res. **21**, 11893–11906 (2014). https://doi.org/10.1007/s11356-014-2592-6
152. P.B. Orr, United States Atomic Energy Commission Unclassified Report ORNL-3271, Oak Ridge, TN, 1962.
153. B. Weaver, F.A. Kappelmann, United States Atomic Energy Commission Unclassified Report ORNL-3559, Oak Ridge, TN, 1964.
154. Weaver, B., Kappelmann, F.A.: Preferential extraction of lanthanides over trivalent actinides by monoacidic organophosphates from carboxylic acids and from mixtures of carboxylic and aminopolyacetic acids. J. Inorg. Nucl. Chem. **30**, 263–272 (1968). https://doi.org/10.1016/0022-1902(68)80089-2

155. Ehnebom, L., Pedersen, B.F.: Molecular and crystal structure of a lanthanide complex, DyDTPA–BMA hydrate. Acta Chem Scand. **46**, 126–130 (1992). https://doi.org/10.3891/acta.chem.scand.46-0126
156. Bligh, S.W.A., Chowdhury, A.H.M.S., Kennedy, D., Luchinat, C., Parigi, G.: Non-ionic bulky Gd(III) DTPA-bisamide complexes as potential contrast agents for magnetic resonance imaging. Magn. Reson. Med. **41**, 767–773 (1999). https://doi.org/10.1002/(SICI)1522-2594(199904)41:4%3c767::AID-MRM16%3e3.0.CO;2-G
157. Lattuada, L., Barge, A., Cravotto, G., Giovenzana, G.B., Teid, L.: The synthesis and application of polyamino polycarboxylic bifunctional chelating agents. Chem. Soc. Rev. **40**, 3019–3049 (2011). https://doi.org/10.1039/c0cs00199f
158. Lammers, H., Maton, F., Pubanz, D., Van Laren, M.W., Van Bekkum, H., Merbach, A.E., Muller, R.N., Peters, J.A.: Structures and dynamics of lanthanide(III) complexes of sugar-based DTP a-bis (amides) in aqueous solution: a multinuclear NMR study. Inorg. Chem. **36**, 2527–2538 (1997). https://doi.org/10.1021/ic961359k
159. Lammers, H., Van Der Heijden, A.M., Van Bekkum, H., Geraldes, C.F.G.C., Peters, J.A.: Multinuclear NMR study of the interactions between the La(III) complex of DTPA-bis(glucamide) and Zn(II) or borate. Inorg. Chim. Acta. **268**, 249–255 (1998). https://doi.org/10.1016/S0020-1693(97)05752-6
160. Heathman, C.R., Grimes, T.S., Zalupski, P.R.: Thermodynamic and spectroscopic studies of trivalent f-element complexation with ethylenediamine-N,N′-di(acetylglycine)-N,N′-diacetic acid. Inorg. Chem. **55**, 2977–2985 (2016). https://doi.org/10.1021/acs.inorgchem.5b02865
161. Aime, S., Botta, M., Fasano, M., Paoletti, S.L., Anelli, P., Uggeri, F., Virtuani, M.: NMR evidence of a long exchange lifetime for the coordinated water in Ln(III)-bis(methylamide)-DTPA complexes (Ln = Gd, Dy). Inorg Chem. **33**, 4707–4711 (1994). https://doi.org/10.1021/ic00099a021
162. Sherry, A.D., Cacheris, W.P., Kuan, K.-T.: Stability constants for Gd3+ binding to model DTPA-conjugates and DTPA-proteins: implications for their use as magnetic resonance contrast agents. Magn. Reson. Med. **8**, 180–190 (1988). https://doi.org/10.1002/mrm.1910080208
163. Geraldes, C.F.G.C., Urbano, A.M., Hoefnagel, M.A., Peters, J.A.: Multinuclear magnetic resonance study of the structure and dynamics of lanthanide(III) complexes of the bis(propylamide) of diethylenetriaminepentaacetic acid in aqueous solution. Inorg. Chem. **32**, 2426–2432 (1993). https://doi.org/10.1021/ic00063a037
164. Aime, S., Benetollo, F., Bombieri, G., Colla, S., Fasano, M., Paoletti, S.: Non-ionic Ln(III) chelates as MRI contrast agents: synthesis, charactetisation and 1H NMR relaxometric investigations of bis(benzylamide)diethylenetriaminepentaacetic acid Lu(III) and Gd(III) complexes. Inorg. Chim. Acta. **254**, 63–70 (1997). https://doi.org/10.1016/s0020-1693(96)05139-0
165. Wang, Y.M., Wang, Y.J., Sheu, R.S., Liu, G.C., Lin, W.C., Liao, J.H.: Relaxivity studies and X-ray structure of Gd(III)-diethylenetriamine-N,N′, N″-triacetic acid-N,N″-bis(2-methoxyphenethylamide) as a potential contrast agent for magnetic resonance imaging. Polyhedron **18**, 1147–1152 (1999). https://doi.org/10.1016/S0277-5387(98)00406-9
166. Annie-Bligh, S.W., Chowdhury, A.H.M.S., McPartlin, M., Scowen, I.J., Bulman, R.A.: Neutral gadolinium(III) complexes of bulky octadentate dtpa derivatives as potential contrast agents for magnetic resonance imaging. Polyhedron **14**, 567–569 (1995). https://doi.org/10.1016/0277-5387(94)00318-9
167. Paul-Roth, C., Raymond, K.N.: Amide functional group contribution to the stability of gadolinium(III) complexes: DTPA derivatives. Inorg. Chem. **34**, 1408–1412 (1995). https://doi.org/10.1021/ic00110a019
168. Wang, Y.M., Cheng, T.H., Liu, G.C., Sheu, R.S.: Synthesis of some N,N ″-bis(amide) derivatives of diethylenetriaminepentaacetic acid and the stabilities of their complexes with Gd3+, Ca2+, Cu2+ and Zn2+. J. Chem. Soc. Dalton Trans. (1997). https://doi.org/10.1039/A605483H
169. Jasanada, F., Nepven, F.: Synthesis of amphiphilic chelating agents : bis(hexadecylamide) and bis(octadecylamide) of diethylenetriaminepentaacetic acid. Tetrahedron Lett. **33**, 5745–5748 (1992). https://doi.org/10.1016/0040-4039(92)89021-4
170. Clough, T.J., Jiang, L., Wong, K.L., Long, N.J.: Ligand design strategies to increase stability of gadolinium-based magnetic resonance imaging contrast agents. Nat. Commun. **10**, 1420–1434 (2019). https://doi.org/10.1038/s41467-019-09342-3
171. Carvalho, J.F., Kim, S.H., Chang, C.A.: Synthesis and metal complex selectivity of macrocyclic DTPA and EDTA bis(amide) ligands. Inorg Chem. **31**, 4065–4068 (1992). https://doi.org/10.1021/ic00046a015
172. Franklin, S.J., Raymond, K.N.: Solution structure and dynamics of lanthanide complexes of the macrocyclic polyamino carboxylate DTPA-dien: NMR study and crystal structures of the lanthanum(III) and europium(III) complexes. Inorg. Chem. **33**, 5794–5804 (1994). https://doi.org/10.1021/ic00103a029
173. Bovens, E., Hoefnagel, M.A., Boers, E., Lammers, H., Van Bekkum, H., Peters, J.A.: Multinuclear magnetic resonance study on the structure and dynamics of lanthanide(III) complexes of cyclic DTPA derivatives in aqueous solution. Inorg. Chem. **35**, 7679–7683 (1996). https://doi.org/10.1021/ic960540q
174. Cacheris, W.P., Quay, S.C., Rocklage, S.M.: The relationship between thermodynamics and the toxicity of gadolinium complexes. Magn. Reson. Imaging. **8**, 467–481 (1990). https://doi.org/10.1016/0730-725X(90)90055-7
175. Imura, H., Choppin, G.R., Cacheris, W.P., De Learie, L.A., Dunn, T.J., White, D.H.: Thermodynamics and NMR studies of DTPA-bis(methoxyethylamide) and its derivatives. Protonation and complexation with Ln(III). Inorg. Chim. Acta. **258**, 227–236 (1997). https://doi.org/10.1016/s0020-1693(96)05522-3
176. Weinmann, H.J., Brasch, R.C., Press, W.R., Wesbey, G.E.: Characteristics of gadolinium-DTPA complex: a potential NMR contrast agent. Am. J. Roentgenol. **142**, 619–624 (1984). https://doi.org/10.2214/ajr.142.3.619
177. Chang, C.A.: Magnetic resonance imaging contrast agents design and physicochemical properties of gadodiamide. Invest Radiol. **28**, 21–27 (1993)
178. Lauffer, R.B.: Paramagnetic metal complexes as water proton relaxation agents for NMR imaging: theory and design. Chem. Rev. **87**, 901–927 (1987). https://doi.org/10.1021/cr00081a003
179. Parker, D., Williams, J.A.G.: Getting excited about lanthanide complexation chemistry. J. Chem. Soc. Dalton Trans. (1996). https://doi.org/10.1039/dt9960003613
180. Gries, H.: Extracellular MRI Contrast Agents Based on Gadolinium. Springer, Berlin, Heidelberg (2002)
181. Tóth, E., Merbach, A.E.: The Chemistry of Contrast Agents in Medical Magnetic Resonance Imaging. Wiley, Chichester (2001)
182. Rothermel, G.L., Rizkalla, E.N., Choppin, G.R.: The kinetics of exchange between a lanthanide ion and the gadolinium complex of N,N″-bis(2-methoxyethylamide-carbamoylmethyl)-diethylenetriamine-N,N′, N″-triacetate. Inorganica Chim. Acta. **262**, 133–138 (1997). https://doi.org/10.1016/S0020-1693(97)05513-8
183. Sarka, L., Burai, L., Király, R., Zékány, L., Brücher, E.: Studies on the kinetic stabilities of the Gd3+ complexes formed with the N-mono(methylamide), N′-mono(methylamide) and

N,N″-bis(methylamide) derivatives of diethylenetriamine-N,N,N′,N″,N″-pentaacetic acid. J. Inorg. Biochem. **91**, 320–326 (2002). https://doi.org/10.1016/S0162-0134(02)00418-X
184. Tóth, É., Burai, L., Brücher, E., Merbach, A.E.: Tuning water-exchange rates on (carboxymethyl)iminobis(ethylenenitrilo) tetraacetate (dtpa)-type gadolinium(III) complexes. J Chem Soc Dalton Trans. (1997). https://doi.org/10.1039/A608505I
185. Jászberényi, Z., Tóth, É., Kálai, T., Király, R., Burai, L., Brücher, E., Merbach, A.E., Hideg, K.: Synthesis and complexation properties of DTPA-N,N″-bis[bis(n-butyl)]-N′-methyl-tris(amide). Kinetic stability and water exchange of its Gd3+ complex. Dalton Trans. (2005). https://doi.org/10.1039/B417272H
186. Jászberényi, Z., Bányai, I., Brücher, E., Király, R., Hideg, K., Kálai, T.: Equilibrium and NMR studies on GdIII, YIII, Cu II and ZnII complexes of various DTPA-N,N″-bis(amide) ligands. Kinetic stabilities of the gadolinium(III) complexes. Dalton Trans. (2006). https://doi.org/10.1039/b514173g
187. Kotek, J., Kálmán, F.K., Hermann, P., Brücher, E., Binnemans, K., Lukeš, I.: Study of thermodynamic and kinetic stability of transition metal and lanthanide complexes of DTPA analogues with a phosphorus acid pendant arm. Eur. J. Inorg. Chem. (2006). https://doi.org/10.1002/ejic.200501114
188. Baranyai, Z., Pálinkás, Z., Uggeri, F., Brücher, E.: Equilibrium studies on the Gd3+, Cu2+ and Zn 2+ complexes of BOPTA, DTPA and DTPA-BMA ligands: kinetics of metal-exchange reactions of [Gd(BOPTA)]2-. Eur. J. Inorg. Chem. (2010). https://doi.org/10.1002/ejic.200901261
189. Sarka, L., Bányai, I., Brücher, E., Király, R., Platzek, J., Radüchel, B., Schmitt-Willich, H.: Synthesis, equilibrium and NMR studies of lanthanide(III) complexes of the N-mono(methylamide) and N ′-mono(methylamide) derivatives of diethylenetriamine-N,N, N ′, N ″, N ″-pentaacetic acid†. J. Chem. Soc. Dalton Trans. (2000). https://doi.org/10.1039/b0052981
190. Sarka, L., Burai, L., Brücher, E.: The rates of the exchange reactions between [Gd(DTPA)]2- and the endogenous ions Cu2+ and Zn2+: a kinetic model for the prediction of the in vivo stability of [Gd(DTPA)]2-, used as a contrast agent in magnetic resonance imaging. Chem. A Eur. J. **6**, 719–724 (2000). https://doi.org/10.1002/(SICI)1521-3765(20000218)6:4%3c719::AID-CHEM719%3e3.0.CO;2-2
191. Zhao, X., Zhuo, R., Lu, Z., Liu, W.: Synthesis, characterization and relaxivity of amphiphilic chelates of DTPA derivatives with GDIII, YbIII and MnII. Polyhedron **16**, 2755–2759 (1997). https://doi.org/10.1016/S0277-5387(97)00029-6
192. P.L. Anelli, I. Bertini, M. Fragai, L. Lattuada, C. Luchinat, G. Parigi, Sulfonamide-functionalized gadolinium DTPA complexes as possible contrast agents for MRI: a relaxometric investigation, Eur. J. Inorg. Chem. (2000). https://doi.org/10.1002/(sici)1099-0682(200004)2000:4<625::aid-ejic625>3.0.co;2-2.
193. Zhang, D.W., Yang, Z.Y., Wang, B.D., Zhang, S.P., Yang, R.D.: Synthesis neutral rare earth complexes of diethylenetriamine-N,N″-bis(acetyl-isoniazid)-N,N′,N″-triacetic acid as potential contrast enhancement agents for magnetic resonance imaging. Chem. Pharm. Bull. **54**, 1203–1206 (2006). https://doi.org/10.1248/cpb.54.1203
194. Dutta, S., Kim, S.-K., Lee, E.J., Kim, T.-J., Kang, D.-S., Chang, Y., Kang, S.O., Han, W.-S.: Synthesis and magnetic relaxation properties of paramagnetic Gd-complexes of new DTPA-bis-amides: The X-ray crystal structure of [Gd(L)(H2O)]•3H_2O (L = DTPA-bis(4-carboxylicphenyl)amide). Bull Korean Chem Soc. **27**, 1038–1042 (2006). https://doi.org/10.5012/bkcs.2006.27.7.1038
195. Dutta, S., Kim, S.K., Patel, D.B., Kim, T.J., Chang, Y.: Some new DTPA-N,N″-bis(amides) functionalized by alkyl carboxylates. Synthesis, complexation and stability properties. Polyhedron **26**, 3799–3809 (2007). https://doi.org/10.1016/j.poly.2007.04.027
196. Martell, A.E., Smith, R.M.: Critical Stability Constants, vol. 1. Plenum, New York (1974)
197. Aime, S., Botta, M., Parker, D., Williams, J.A.G.: Nuclear magnetic resonance studies of neutral lanthanide(III) complexes with tetraaza-macrocyclic ligands containing three phosphinate and one carboxamide co-ordinating arms. J. Chem. Soc. Dalton Trans. (1995). https://doi.org/10.1039/DT9950002259
198. Choppin, G.R., Baisden, P.A., Khan, S.A.: Nuclear magnetic resonance studies of diamagnetic metal-diethylenetriaminepentaacetate complexes. Inorg. Chem. **18**, 1330–1332 (1979). https://doi.org/10.1021/ic50195a033
199. Gries, H., Miklautz, H.: Some physicochemical properties of the gadolinium-DTPA complex, a contrast agent for MRI. Physiol. Chem. Phys. Med NMR. **16**, 105–112 (1984)
200. Stezowski, J.J., Hoard, J.L.: Heavy metal ionophores: correlations among structural parameters of complexed nonpeptide polyamino acids. Isr. J. Chem. **24**, 323–334 (1984). https://doi.org/10.1002/ijch.198400055
201. Peters, J.A.: Multinuclear NMR study of lanthanide(III) complexes of diethylenetriaminepentaacetate. Inorg. Chem. **27**, 4686–4691 (1988). https://doi.org/10.1021/ic00299a003
202. Aime, S., Botta, M.: Solution structure and dynamics of DTPA-Ln(III) complexes (DTPA=diethylene triamine penta acetate; LnLa, Pr, Eu). Inorg. Chim. Acta. **177**, 101–105 (1990). https://doi.org/10.1016/S0020-1693(00)91917-0
203. Wang, J., Gao, G., Zhang, Z., Zhang, X., Wang, Y.: Syntheses and structural determinations of the nine-coordinate rare earth metal: Na_4[DyIII(dtpa)(H_2O)]$_2$·16H_2O, Na[DyIII(edta)(H_2O)$_3$]·3.25H_2O and Na_3[DyIII(nta)$_2$(H_2O)]·5.5H_2O. J. Coord. Chem. **60**, 2221–2241 (2007). https://doi.org/10.1080/00958970701258622
204. Liu, B., Wang, Y.F., Wang, J., Gao, J., Xu, R., Kong, Y.M., Zhang, L.Q., Zhang, X.D.: Syntheses and crystal structures of nine-coordinate K2[EuIII(dtpa)(H_2O)]·5H_2O and Na_2[TbIII(Httha)]·6H_2O complexes. J. Struct. Chem. **50**, 880–886 (2009). https://doi.org/10.1007/s10947-009-0131-y
205. Fusaro, L., Mocci, F., Muller, R.N., Luhmer, M.: Insight into the dynamics of lanthanide-DTPA complexes as revealed by oxygen-17 NMR. Inorg. Chem. **51**, 8455–8461 (2012). https://doi.org/10.1021/ic3010085
206. Babailov, S.P.: Thulium diketonate as NMR paramagnetic probe for moderately fast molecular dynamics and supersensitive reagent for in situ control of temperature. Sens. Actuators B Chem. **233**, 476–478 (2016). https://doi.org/10.1016/j.snb.2016.04.009
207. Babailov, S.P.: Lanthanides as NMR/MRI temperature sensors and probes of moderately fast molecular dynamics in aqueous medium: a dependence of activation energy of racemization in complexes of diethylenetriaminepentaacetat on lanthanide ion. Sens. Actuators B Chem. **251**, 108–111 (2017). https://doi.org/10.1016/j.snb.2017.05.033